Electron-Transfer Activation in the Thermal and Photochemical Osmylations of Aromatic EDA Complexes with Osmium(VIII) Tetroxide

J. M. Wallis and J. K. Kochi*

Contribution from the Department of Chemistry, University of Houston, University Park, Houston, Texas 77204. *Received May 9, 1988*

Abstract: Various types of arenes (Ar) spontaneously form with osmium tetroxide a series of highly colored solutions of electron donor–acceptor or EDA complexes such as [Ar,OsO_4] in nonpolar solvents. Charge-transfer or *CT osmylation* is simply effected by the actinic irradiation of the absorption bands ($h\nu_{CT}$), and the molecular structures of the OsO_4 adducts of benzene (**B**) and anthracene (**A**) are elucidated by X-ray crystallography. The metastable ion pair [Ar^+, OsO_4^-] is established as the seminal intermediate in *CT osmylation* by time-resolved picosecond spectroscopy attendant upon the specific excitation of the EDA complex. According to Scheme II, the rapid collapse of the ion pair (eq 16) with a rate constant $k \sim 10^9\ s^{-1}$ represents the critical transformation in adduct formation. Importantly, this ion-pair mechanism accommodates (a) the osmylation of a wide range of arene donors from the mononuclear benzenes to the electron-rich polycyclic arenes (Table V) under the common umbrella of photoexcitation and (b) the profound effect on the regiochemistry of anthracene (Table VI) by subtle variations in solvent polarity. In the absence of deliberate irradiation (i.e., in the dark), the EDA complexes of OsO_4 with electron-rich arenes, especially the polynuclear naphthalene, anthracene and phenanthrene, slowly undergo the direct thermal or *DT osmylation* to yield the same series of adducts. As such, there is a close relationship between the photoexcited state leading to CT osmylation and the activated complex in DT osmylation. Indeed the formation of the highly unusual adduct **A** by OsO_4 addition to the terminal ring of anthracene binds in common the transition state for DT osmylation and the ion-pair collapse in CT osmylation. Thus the electron-transfer mechanism in Scheme IV employs the adiabatic ion pair (eq 20) to account for the same regiospecificities in DT osmylations. Such a unified view of arene osmylation can be extended to the promoted thermal or *PT osmylation* via the five-coordinate OsO_4(py), as commonly practiced for bis-hydroxylation of alkenes.

Oxo-metals have drawn increased attention as viable oxidation catalysts for various types of oxygen-atom transfers to organic and biochemical substrates.[1,2] However only scant mechanistic understanding exists of the oxidation pathways, certainly with respect to the nature of the activation barrier and the identification of the reactive intermediate(s). Among oxo-metals, osmium tetroxide is a particularly intriguing oxidant since it is known to rapidly oxidize various types of alkenes, but it nonetheless eschews the electron-rich aromatic hydrocarbons like benzene and naphthalene.[3-7] Such selectivities do not obviously derive from differences in the donor properties of the hydrocarbons since the oxidation (ionization) potentials of arenes are actually less than those of alkenes.[8] The similarity in the electronic interactions of arenes and alkenes toward osmium tetroxide relates to the series of electron donor–acceptor (EDA) complexes formed with both types of hydrocarbons, i.e.[9-11]

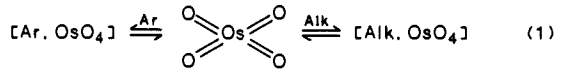

(1)

Common to both arenes and alkenes is the immediate appearance of similar colors that are diagnostic of charge-transfer (CT) absorptions arising from the electronic excitation ($h\nu_{CT}$) of the EDA complexes formed in eq 1.[12,13] As such, the similarity in the color changes point to electronic interactions in the arene complex [Ar, OsO_4] that mirror those extant in the alkene complex [Alk, OsO_4].[14]

The charge-transfer colors of the alkene EDA complexes are fleeting, and they are not usually observed owing to the rapid followup rate of osmylation,[9,14c] i.e.

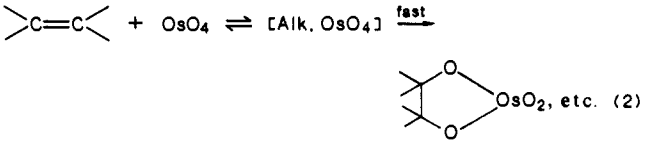

(2)

By contrast, simple (monocyclic) arenes do not afford thermal adducts with osmium tetroxide, benzene actually being a most desirable solvent for alkene hydroxylation.[15] However, with some extended polynuclear aromatic hydrocarbons such as benzpyrene, dibenzanthracene, and cholanthrene, a thermal reaction does lead to multiple osmate adducts and finally to polyhydric alcohols.[16,17] Tricyclic aromatic hydrocarbons such as phenanthrene show in-

(1) *Organic Synthesis by Oxidation with Metal Compounds*; Mijs, W. J.; de Jonge, C. R. H. I., Eds.; Plenum: New York, 1986. See, also: Holm, R. H. *Chem. Rev.* **1987**, *87*, 1401.
(2) Sheldon, R. A.; Kochi, J. K. *Metal-Catalyzed Oxidations of Organic Compounds*; Academic: New York, 1981.
(3) (a) Hofmann, K. A. *Chem. Ber.* **1912**, *45*, 3329. (b) Hofmann, K. A.; Ehrhart, O.; Schneider, O. *Chem. Ber.* **1913**, *46*, 1657.
(4) (a) Criegee, R. *Liebigs Ann.* **1936**, *522*, 75. (b) Criegee, R.; Marchand, B.; Wannowius, H. *Liebigs Ann.* **1942**, *550*, 99.
(5) Schröder, M. *Chem. Rev.* **1980**, *80*, 187.
(6) Griffith, W. P. *Chemistry of the Rarer Platinum Metals (Os, Ru, Ir and Rh)*; Wiley Interscience: New York, 1967.
(7) (a) Livingstone, S. E. *Comprehensive Inorganic Chemistry*; "Chemistry of Ruthenium, Rhodium Palladium, Osmium, Iridium and Platinum", Pergamon: New York, 1973; Chapter 43. (b) Heaton, B. T. In *Annual Reports Inorganic and General Syntheses*; Niedenzu, K., Zimmer, H., Eds.; Academic: New York, 1974.
(8) For leading references, see: Fukuzumi, S.; Kochi, J. K. *J. Am. Chem. Soc.* **1982**, *104*, 7599.
(9) Nugent, W. A. *J. Org. Chem.* **1980**, *45*, 4533.
(10) Hammond, P. R.; Lake, R. R. *J. Chem. Soc. A* **1971**, 3819.
(11) Burkhardt, L. A.; Hammond, P. R.; Knipe, R. H.; Lake, R. R. *J. Chem. Soc. A* **1971**, 3789.
(12) Foster, R. F. *Charge-Transfer Complexes in Organic Chemistry*; Academic: New York, 1969.
(13) Andrews, L. J.; Keefer, R. M. *Molecular Complexes in Organic Chemistry*; Holden-Day: San Francisco, 1964.
(14) (a) Hanna, M. W.; Lippert, J. L. In *Molecular Complexes*; Foster, R., Ed.; Crane, Russak & Co.: New York, 1973; Chapter I. (b) The implications of a common CT relationship of arene and alkene donors toward the same electrophile (bromine) was established earlier. See: Fukuzumi, S.; Kochi, J. K. *J. Am. Chem. Soc.* **1982**, *104*, 7599. (c) For a discussion of EDA complexes as obligatory intermediates, see: footnotes 19 and 20 in Fukuzumi et al. (Fukuzumi, S.; Kochi, J. K. *J. Am. Chem. Soc.* **1980**, *102*, 2141).
(15) Fieser, L. F.; Fieser, M. *Reagents for Organic Synthesis*; Wiley: New York, 1967–1985.
(16) (a) Cook, J. W.; Schoental, R. *J. Chem. Soc.* **1948**, 170. (b) Cook, J. W.; Loudon, J. D.; Williamson, W. F. *J. Chem. Soc.* **1950**, 911.
(17) (a) Criegee, R.; Höger, E.; Huber, G.; Knick, P.; Marktscheffel, F.; Schellenberger, H. *Liebigs Ann.* **1956**, *599*, 81.

0002-7863/88/1510-8207$01.50/0

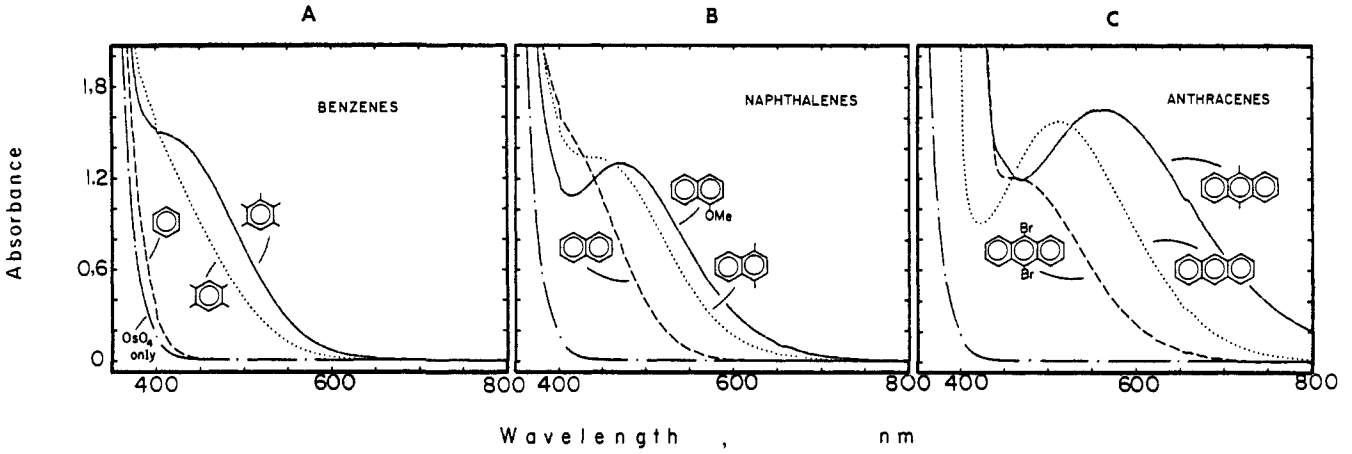

Figure 1. Charge-transfer absorption bands from dichloromethane solutions containing 0.1 M OsO_4 and (A) 0.1 M benzene, durene, and pentamethylbenzene; (B) 0.1 M naphthalene, 1,4-dimethylnaphthalene, and 1-methoxynaphthalene; (C) 0.05 M 9,10-dibromoanthracene (×2), 0.1 M anthracene, and 9,10-dimethylanthracene.

termediate reactivity with osmium tetroxide to afford (over several weeks) the 1:1 adduct, i.e.[4b,16a]

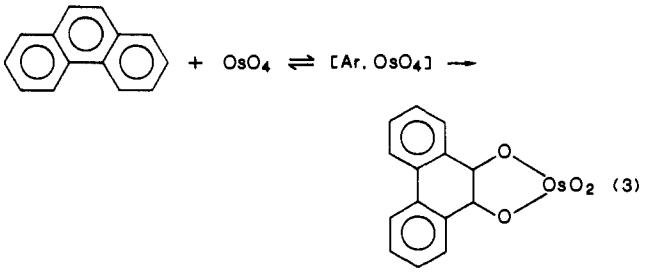

Osmylation in eq 3 occurs at the HOMO site of the arene in a manner analogous to that observed in alkene osmylations (eq 2). In this context, anthracene is a particularly noteworthy substrate since it is purported to afford an unusual 2:1 adduct by oxidative attack at a terminal ring in preference to the most reactive meso (9,10-) positions.[18]

We believe that the inextensible range of arene reactivities offers the unique opportunity to probe the mechanism of osmium tetroxide oxidations for four principal reasons. First, the EDA complexes in eq 1 relate alkenes directly to arenes via the oxo-metal interactions in the precursors relevant to oxidation. Second, the thermal osmylation of polynuclear arenes (see eq 3) has an exact counterpart in the photostimulated osmylations that are widely applicable to even such otherwise inactive arenes as benzene.[19] Since this charge-transfer process is readily associated with excitation ($h\nu_{CT}$) of the EDA complex to the ion pair, i.e.

$$[Ar, OsO_4] \xrightleftharpoons{h\nu_{CT}} [Ar^{\bullet+}, OsO_4^{\bullet-}] \xrightarrow{fast} \text{adduct} \qquad (4)$$

it is hereafter referred to simply as charge-transfer osmylation. Third, the dual pathways of *thermal* and *charge-transfer* osmylation allow the regio- and stereochemistry for OsO_4 addition to be quantitatively compared, especially in the OsO_4 adducts of the polycyclic arenes: phenanthrene, anthracene, and naphthalene. Fourth, the activation process for CT osmylation can be unambiguously established by the application of time-resolved (picosecond) spectroscopy for direct observation of the reactive intermediates, as previously defined in other aromatic CT processes.[20] Accordingly, our initial task in this study is to establish the common CT character of the EDA complexes of OsO_4 with the arene series (benzene, naphthalene, and anthracene) as well as the structural elucidation of their OsO_4 adducts by X-ray crystallographic and spectral analyses.

Table I. Charge-Transfer Absorption Spectra of the EDA Complexes of Various Arenes and Osmium Tetroxide[a]

arene	IP (eV)	solvent n-C_6H_{14}	CCl_4	CH_2Cl_2
benzene	9.23[b]	*h*	*h*	*h*
mesitylene	8.42[b]	390	395	*h*
durene	8.05[b]	398	402	*h*
naphthalene	8.12[c]	416	426	*h*
phenanthrene	8.1[c]	~406	418	*h*
hexamethylbenzene	7.85[b]	474	472	442
1,4-dimethylnaphthalene	7.78[d]	468	474	~450
1-methoxynaphthalene	7.72[e]	484	492	470
2,6-dimethoxynaphthalene	7.58[f]	516	524	490
anthracene	7.43[g]	520	532	510
9-methylanthracene	7.25[g]	548	558	530
9-bromoanthracene	7.47[g]	496	508	490
9,10-dibromoanthracene	7.54[g]	468	486	~466
9,10-dimethylanthracene	7.11[g]	576	578	556

[a] In solutions of 0.1 M arene and 10^{-2} M OsO_4 at 25 °C. [b] Reference 21. [c] Reference 22. [d] Reference 23a. [e] Reference 23b. [f] Reference 23c. [g] Reference 24. [h] λ_{max} obscured.

Results

I. Charge-Transfer Complexes of OsO_4 with Benzenes, Naphthalenes, and Anthracenes. A colorless solution of osmium tetroxide in *n*-hexane or dichloromethane upon exposure to benzene turned yellow instantaneously. With durene an orange coloration developed, and a clear bright red solution resulted from hexamethylbenzene. The progressive change in color from dark yellow, yellow-orange, to orange characterized the binuclear aromatic series: naphthalene, 1,4-dimethylnaphthalene, and 1-methoxynaphthalene under the same conditions. With the family of anthracenes, the 9,10-dibromo derivative immediately developed an orange color with OsO_4, whereas the parent hydrocarbon and the 9,10-dimethyl analogue afforded purple- and mauve-colored solutions, respectively.

The quantitative effects of these dramatic color changes are illustrated in Figure 1 by the spectral shifts of the electronic absorption bands that accompanied the variations in aromatic conjugation and substituents. For example, the yellow color from benzene appeared as a nondescript shift of the end absorption of OsO_4 to beyond 380 nm in Figure 1A. The marked spectral change with naphthalene was noted as the absorption band with a shoulder at $\lambda \sim 420$ nm in Figure 1B. Finally the anthracene color constituted a distinctive new absorption band in Figure 1C with $\lambda_{max} = 510$ nm. Such a progressive bathochromic shift parallels the decrease in the arene ionization potentials (IP) in the following order: benzene 9.23 eV, naphthalene 8.12 eV,

(18) Cook, J. W.; Schoental, R. *Nature (London)* **1948**, *161*, 237.
(19) Wallis, J. M.; Kochi, J. K. *J. Org. Chem.* **1988**, *53*, 1679.
(20) (a) Hilinski, E. F.; Masnovi, J. M.; Kochi, J. K.; Rentzepis, P. M. *J. Am. Chem. Soc.* **1984**, *106*, 8071. (b) Mataga, N. *Pure Appl. Chem.* **1984**, *15*, 1255. Masnovi, J. M.; Korp, J. D.; Kochi, J. K. *J. Phys. Chem.* **1985**, *89*, 5387. (c) Masnovi, J. M.; Huffman, S. C.; Kochi, J. K.; Hilinski, E. F.; Rentzepis, P. M. *Chem. Phys. Lett.* **1984**, *106*, 20.

anthracene 7.43 eV.[21-24] Indeed the general relationship between the spectral band energy and the ionization potential applies to all the substituted arenes examined in this study (Table I). In particular, increasing the number of methyl groups in benzene to durene and pentamethylbenzene resulted in a gradual red shift[25] of the new absorption bands as clearly defined in Figure 1A. The same trend was observed with the naphthalenes and anthracenes. Furthermore methoxy and bromo substituents have diametrically opposed effects as illustrated in Figure 1 (parts B and C, respectively) in accord with their electron-releasing and electron-withdrawing properties on the arene IPs (Table I).[26] Such spectral behaviors are diagnostic of electron donor–acceptor complexes such as those formed in eq 1. According to Mulliken,[27] the new absorption bands derive from charge-transfer excitation ($h\nu_{CT}$ in eq 4) with the energetics defined by[12]

$$h\nu_{CT} = IP - E_A - \omega \quad (5)$$

where E_A is the electron affinity of the OsO_4 acceptor and ω is the dissociation energy of the CT excited ion-pair state. The empirical plot that is illustrated in Figure 2 defines the linear relationship

$$h\nu_{CT} = 0.85IP - 3.92 \quad (6)$$

with the reasonable correlation coefficient of $r = 0.95$. It accords quantitatively with eq 5 in which E_A is perforce constant for the common OsO_4 acceptor, and ω is within the experimental scatter relatively invariant for structurally related arene donors.[28] Table I includes the charge-transfer absorption bands of the arene–OsO_4 complexes in three typical solvents, *n*-hexane, carbon tetrachloride, and dichloromethane with dielectric constants of 1.89, 2.24, and 9.08, respectively.[29] The slight blue-shift of λ_{CT} that consistently accompanied the solvent change from hexane to the more polar dichloromethane is a spectral feature that has been noted with a variety of other EDA complexes.[30]

The formation constants K for the arene–OsO_4 complexes were evaluated in a pair of typical solvents (Table II) by the spectrophotometric procedure of Benesi and Hildebrand,[31] i.e.

$$\frac{[OsO_4]}{A_{CT}} = \frac{1}{K\epsilon_{CT}[Ar]} + \frac{1}{\epsilon_{CT}} \quad (7)$$

where A_{CT} is the molar absorbance and ϵ_{CT} the extinction coefficient of the CT band at the monitoring wavelength under conditions where $[Ar] \gg [OsO_4]$. Owing to the limited values of K however, a small negative intercept (ϵ_{CT}^{-1}) often resulted from an otherwise excellent linear fit of the experimental data ($r > 0.99$). This graphical feature has been previously noted by Hammond,[10] and it largely vitiates a quantitative determination of the formation constant of weak EDA complexes.[32] Accordingly, to emphasize the uniformity of the three classes of arenes examined in this study, we merely list the values of the product $K\epsilon_{CT}$ in Table II.[33] Indeed the colored complexes are so weak

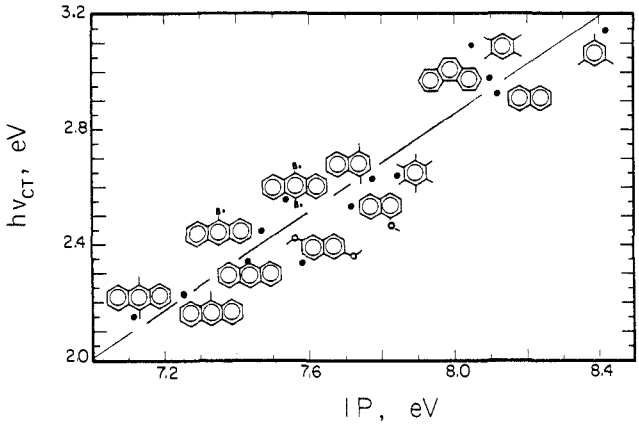

Figure 2. General correlation of the CT transition energy ($h\nu_{CT}$) of the arene–OsO_4 complexes in CCl_4 with the ionization potential of various arenes as indicated.

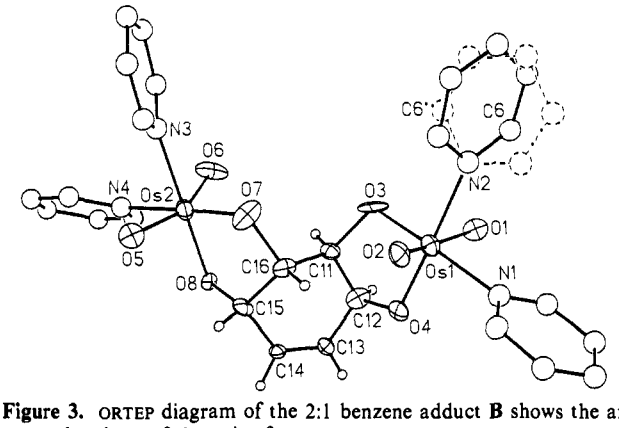

Figure 3. ORTEP diagram of the 2:1 benzene adduct **B** shows the anti stereochemistry of the pair of osmate esters.

that all attempts at isolation, including the freezing of various mixtures of OsO_4 in neat aromatic donors, merely led to phase separation and discharge of color.[10] Thus the absorption bands are properly ascribed to contact charge transfer.[34] It is also noteworthy that solutions of OsO_4 and aromatic donors exhibited new CT absorption bands only in highly nonpolar solvents such as alkanes and chloroalkanes. In the more polar solvents acetone, dioxane, or acetonitrile, no new absorption bands could be discerned. Similarly upon the addition of small amounts of pyridine to a hexane solution of OsO_4 and arene, the CT colors were immediately discharged, undoubtedly due to the preferential coordination of the Lewis base with the acceptor.[35]

$$OsO_4 \overset{py}{\rightleftharpoons} OsO_4(py) \quad (8)$$

II. Molecular Structures of the OsO_4 Adducts to Benzene, Naphthalene, and Anthracene. The elucidation of the OsO_4 adducts from each class of arene was critically important to thermal as well as charge-transfer osmylations, and their structures are thus presented individually below.

Benzene adduct was obtained as a deep brown amorphous solid from the charge-transfer osmylation (vide infra) in hexane.[19] Owing to the insolubility of this material, it was immediately converted to the pyridine derivative **B** with the composition $(C_6H_6)(OsO_4)_2(py)_4$ established by elemental analysis.[36] The

(21) Howell, J. O.; Goncalves, J. M.; Amatore, C.; Klasinc, L.; Wightman, R. M.; Kochi, J. K. *J. Am. Chem. Soc.* **1984**, *106*, 3968.
(22) *Handbook of Chemistry and Physics*; Weast, R. C., Ed.; CRC Press: Cleveland, OH, 1974. See also ref 27b.
(23) (a) Nounou, P. *J. Chim. Phys.* **1966**, *63*, 994. (b) Bock, H.; Wagner, G.; Kroner, J. *Chem. Ber.* **1972**, *105*, 3850. (c) Nagy, O. S.; Dupire, S.; Nagy, J. B. *Tetrahedron* **1975**, *31*, 2453.
(24) Masnovi, J. M.; Seddon, E. A.; Kochi, J. K. *Can. J. Chem.* **1984**, *62*, 2552.
(25) Heilbronner, E.; Maier, J. P. In *Electron Spectroscopy*; Brundle, C. R., Baker, A. D., Eds.; Academic: New York, 1977, Vol. I, p 250 ff.
(26) Lowry, T. H.; Richardson, K. S. *Mechanism and Theory in Organic Chemistry*; Harper and Row: New York, 1981.
(27) (a) Mulliken, R. S. *J. Am. Chem. Soc.* **1952**, *74*, 811. (b) Mulliken, R. S.; Person, W. B. *Molecular Complexes, A Lecture and Reprint Volume*; Wiley: New York, 1969.
(28) For a recent discussion, see ref 17 and 21, and Klingler et al. (Klingler, R. S.; Fukuzumi, S.; Kochi, J. K. *Inorganic Chemistry: Toward the 21st Century*; ACS Symposium Series 211; American Chemical Society: Washington, DC, 1983).
(29) Dean, J. A. *Lange's Handbook of Chemistry*, XIII ed.; McGraw-Hill Book Co.: New York, 1985.
(30) Foster, R. F. Chapter 12 in ref 12.
(31) Benesi, H. A.; Hildebrand, J. H. *J. Am. Chem. Soc.* **1949**, *71*, 2703.
(32) See: Foster, R. F. *Molecular Complexes* **1974**, *2*, 107.
(33) The value of $K \sim 0.3$ M^{-1} for arenes[19] compares with 48 M^{-1} for the formation of $OsO_4(py)$ in eq 8. See Supplementary Material Available for Table II.
(34) Tamres, M.; Strong, R. L. *Molecular Association*; Foster, R. F., Ed.; Academic: New York: 1979; Vol. II, p 331 ff.
(35) (a) Hair, M. L.; Robinson, P. L. *J. Chem. Soc.* **1958**, 106; **1960**, 2775. (b) Cleare, M. J.; Hydes, P. C.; Griffith, W. P.; Wright, M. J. *J. Chem. Soc., Dalton Trans.* **1977**, 941. (c) Griffith, W. P.; Skapski, A. C.; Woode, K. A.; Wright, M. J. *Inorg. Chim. Acta* **1978**, L413. (d) Tschugajett, L.; Tschernjajett, J. *Z. Anorg. Chem.* **1928**, *172*, 216.
(36) Elemental analysis by Atlantic Microlabs, Inc., Atlanta, GA.

infrared spectrum of the 2:1 adduct **B** revealed a strong band at 828 cm^{-1} diagnostic of the *trans*-dioxoosmium moiety O=Os=O.[37] The pyridine ligands appeared in the ^1H NMR spectrum of **B** as three resonances at δ 8.92, 7.83, and 7.44 in a characteristic 8:4:8 intensity ratio for the α, γ, and β protons, respectively.[38] These diagnostic resonances were used to calibrate the remaining ^1H resonances at δ 6.12 (d, 2 H) and 5.17 (m, 4 H) for the unique pair of olefinic protons and the pairs of inequivalent hydrogens bound to carbon atoms bearing the two osmate groups, respectively, in the structure shown below. In order to establish the

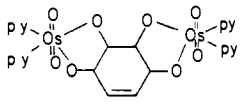

B

osmate stereochemistry, we attempted to grow a single crystal of **B** for X-ray crystallography. Since our repeated and varied attempts yielded only unsuitable microcrystals, we synthesized **B** by an independent route. Thus *cis*-1,2-dihydrocatechol was first converted to the mono-osmate ester $\mathbf{B_1}$ in 70% yield by a standard esterification procedure described in eq 9a.[39] One of the remaining

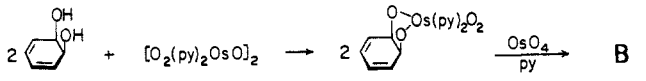

(9a,b)

double bonds in $\mathbf{B_1}$ was then thermally osmylated in eq 9b by treatment with 1 equiv of OsO_4 in dichloromethane containing 2 equiv of pyridine at 25 °C to afford a new sample of **B** that was spectrally identical with the 2:1 adduct obtained via CT osmylation (vide supra). Unlike the latter however, the careful crystallization of the sample prepared via eq 9 led to a dark brown, monoclinic crystal of **B**.[40] The ORTEP diagram in Figure 3 obtained from the single crystal of **B** shows the skew-boat conformation of the cyclohexene skeleton and the pair of osmate esters in an anti relationship above and below the six-membered ring. Both osmium(VI) atoms are octahedral with each pyridine trans to a bridging μ-oxo ligand so that the N–Os–O angle was close to the ideal 180°. The two terminal oxo ligands were however significantly distorted away from this ideal angle at 163 and 158°, as previously noted in related structures.[41,42] The 2:1 adduct could be further transformed into the 3:1 adduct **B′** by treatment with another equivalent of OsO_4 and pyridine.

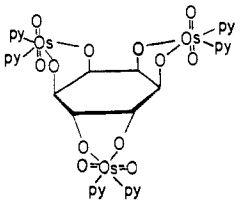

B′

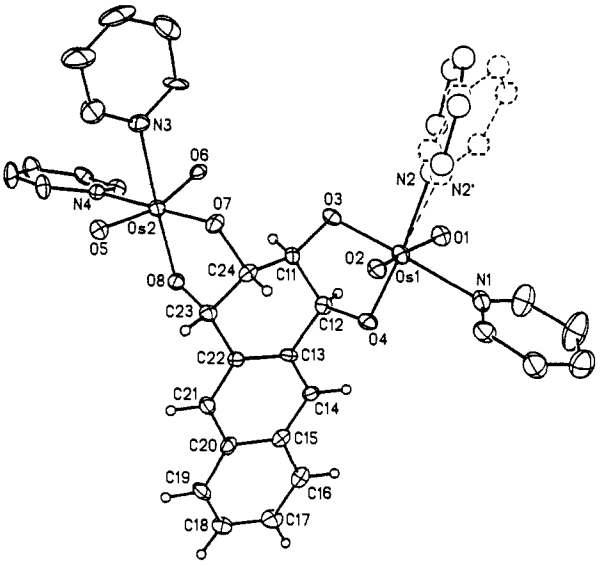

Figure 4. ORTEP diagram of the 2:1 adduct **A** showing the addition of two OsO_4 with anti stereochemistry to the terminal ring of anthracene.

Anthracene adduct A was obtained as dark brown crystals from the thermal osmylation (vide infra) with 2 equiv of OsO_4 in benzene solution containing 4 equiv of pyridine. The 2:1 stoichiometry $(C_{14}H_{10})(OsO_4)_2(py)_4$ was established for **A** by elemental analysis, and the infrared and ^1H NMR spectra revealed the strong band at 834 cm^{-1} of the *trans*-dioxoosmium moiety and the two pairs of coordinated pyridine ligands analogous to those observed in the benzene adduct **B**. The diagnostic pyridine resonances in the ^1H NMR spectrum of **A** were used to calibrate (vide supra) the remaining aromatic resonances as multiplets at δ 7.33 (2 H) and 7.80 (2 H) together with a unique, sharp singlet at δ 8.04 (2 H). The protons attached to the carbon atoms bearing the two osmate groups appeared as a pair of 1:1 doublets at δ 5.25 (2 H) and 5.90 (2 H). The absence of ^1H resonances assignable to olefinic C–H bonds and the appearance of the unique singlet (suggestive of the meso protons of anthracene[18]) supported a 2:1 adduct at the terminal ring, i.e.

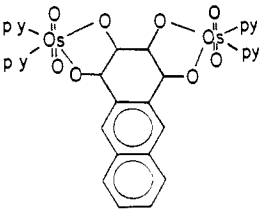

A

This structure thus accords with the earlier formulation based on degradative studies.[18] Nonetheless the critical importance of the anthracene adduct necessitated its structural confirmation by the single-crystal determination (see Experimental Section) illustrated in Figure 4. The ORTEP diagram of **A** shows the pair of osmate esters on the terminal ring to occupy the same anti stereochemical relationship as that found in the benzene adduct **B**. Indeed the bond lengths and angles in the osymlated six-membered rings of **A** and **B** bear a strong structural similarity to each other (see Experimental Section).

Phenanthrene adduct P from the thermal osmylation (vide infra) was obtained as the 1:1 adduct $(C_{14}H_{10})(OsO_4)(py)_2$, as established by elemental analysis.[36] The molecular structure of **P** could be readily characterized solely by spectroscopic methods without recourse to X-ray crystallography. Thus the presence of the *trans*-dioxoosmium(VI) moiety was revealed by the strong IR band at 834 cm^{-1}, and the pair of associated pyridine ligands appeared as the characteristic set of three resonances at δ 8.86, 7.72, and 7.43 with the intensity ratio of 4:2:4 for the α, γ, and β protons, respectively. The latter was used to calibrate the remaining ^1H

(37) (a) Griffith, W. P. *Coord. Chem. Rev.* **1970**, *5*, 459. (b) Marzilli, L. G.; Hanson, B. E.; Kistenmacher, T. J.; Epps, L. A.; Stewart, R. C. *Inorg. Chem.* **1976**, *15*, 1661.

(38) (a) Subbaraman, L. R.; Subbaraman, J.; Behrmann, E. J. *Inorg. Chem.* **1972**, *11*, 2621; (b) Subbaraman, L. R.; Subbaraman, J.; Behrmann, E. J. *Bioinorg. Chem.* **1971**, *1*, 35.

(39) (a) Subbaraman, L. R.; Subbaraman, J.; Behrmann, E. J. *J. Org. Chem.* **1973**, *38*, 1499. (b) Griffith, W. P.; Rossetti, R. *J. Chem. Soc., Dalton Trans.* **1972**, 1449. See also ref 4b.

(40) The difference probably lies in a slight impurity of the syn isomer of B prepared from the CT osmylation.

(41) (a) Cartwright, B. A.; Griffith, W. P.; Schröder, M.; Skapski, A. C. *Inorg. Chim. Acta* **1981**, *53*, L129. (b) Cartwright, B. A.; Griffith, W. P.; Schröder, M.; Skapski, A. C. *J. Chem. Soc., Chem. Commun.* **1978**, 853. (c) Gulliver, D. J.; Levason, W. *Coord. Chem. Rev.* **1982**, *46*, 1.

(42) (a) Conn, J. F.; Kim, J. J.; Suddath, F. L.; Blattmann, P.; Rich, A. *J. Am. Chem. Soc.* **1974**, *96*, 7152. (b) Neidle, S.; Stuart, D. I. *Biochim. Biophys. Acta* **1976**, *418*, 226. (c) Prangé, T.; Pascard, C. *Acta Crystallogr.* **1977**, *B33*, 621.

Table III. Direct Thermal (DT) Osmylation of Polycyclic Arenes with OsO_4[a]

arene	(M)	solvent	temp (°C)	time (h)	adduct	conv,[b] (%)
phenanthrene	(0.10)	*n*-C_6H_{14}	25	1032	P	7
anthracene	(0.037)	*n*-C_6H_{14}	25	1224	A[d,e]	10
anthracene	(0.085)	*n*-C_7H_{16}[c]	100	31	A[d,f]	68
naphthalene	(0.12)	*n*-C_7H_{16}[c]	100	132	N[d,g]	3
1,4-dimethyl-naphthalene	(0.048)	*n*-C_6H_{14}	25	1224	N_{m2}[h]	8

[a] In 5 mL of solvent containing 2 equiv of OsO_4 only and subsequent treatment to the pyridine derivative. [b] Conversion to the combined isomers (as applicable) based on Ar charged (see footnote 43). [c] In a sealed tube. [d] Mixture of anti/syn isomers (see text). [e] 60/40. [f] 67/33. [g] 21/79. [h] 1,4-Dimethyl analogue of *N* as a single isomer.

resonances at δ 7.84 (2 H), 7.66 (2 H), and 7.33 (4 H) for the biphenyl moiety as well as the unique singlet at δ 5.42 (2 H) for the pair of equivalent protons bound to the osmate-bearing carbon in the structure below. This structure thus accords with that proposed earlier by Criegee and co-workers,[4b] based on the hydrolysis of the osmate followed by dehydration to 9-phenanthrol.

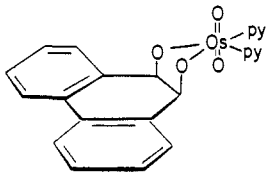

P

Naphthalene adduct N from the thermal osmylation with a mixture of OsO_4 and pyridine consisted of the 2:1 adduct $(C_{10}H_8)(OsO_4)_2(py)_4$ by elemental analysis. The infrared and ^1H NMR spectrum of N revealed the characteristic band at 833 cm^{-1} of the *trans*-O=Os=O moiety, and the two pairs of coordinated pyridines as described above. The latter was used to calibrate the two aromatic resonances at δ 7.54 (2 H) and 7.80 (2 H). The protons attached to the osmylated positions appeared as doublets at δ 5.22 (2 H) and 5.75 (2 H) in the ^1H NMR spectrum and as two singlets at δ 89.6 and 87.3 in the $^{13}C\{^1H\}$ NMR spectrum. These pairs of resonances suggested N to have a structure with C_2 or C_s symmetry, as required for the bis-osmylation of a single naphthalene ring, i.e.

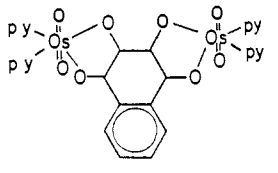

N

By analogy with the benzene adduct **B** (Figure 3) and the anthracene adduct **A** (Figure 4), we infer that the naphthalene adduct N has the same anti stereochemistry for the pair of osmate esters.

III. Thermal Osmylation of Naphthalene, Anthracene, and Phenanthrene. Benzene showed no signs of osmylation in the absence of light, as indicated by the persistence of the yellow color of the [C_6H_6, OsO_4] complex in *n*-hexane even upon prolonged standing. On the other hand, the orange CT color of the phenanthrene complex [$C_{14}H_{10}$, OsO_4] slowly diminished over a period of weeks, accompanied by the formation of a dark brown precipitate of the composition ($C_{14}H_{10}OsO_4$). Dissolution of the solid in pyridine yielded the 1:1 adduct ($C_{14}H_{10}OsO_4py_2$) **P** as the sole product in very low conversion (Table III).[43] Anthracene behaved similarly to afford the 2:1 adduct in 10% conversion only after 2 months. The thermal osymlation could be expedited in a purple solution of refluxing *n*-heptane (100 °C) to effect a 68% conversion in 30 h. However even at these relatively elevated temperatures, naphthalene was converted to the corresponding 2:1 adduct to only a limited extent (entry 4, Table III). In every case, the dark brown primary adducts were easily collected from the reaction mixture as insoluble solids and then immediately ligated with pyridine for structural characterization, as presented above. Indeed we found that the characteristic IR and ^1H NMR spectra of the anthracene, phenanthrene, and naphthalene adducts such as **A**, **P**, and **N**, respectively, allowed the ready analysis of the osmylated adducts listed in Table III (see the Experimental Section for details). Since these adducts were derived from the arenes with only OsO_4 present, the chemical transformation is hereinafter designated as the DIRECT THERMAL or DT osmylation.

For comparison, we also osmylated the same polynuclear arenes in the presence of promoter bases, typically pyridine.[44] Under these conditions, the adducts **A**, **P**, and **N** were formed directly in the reaction mixture and at substantially increased rates of reaction, as previously established with the related family of alkene substrates.[45] Such a procedure differs visually from the DT osmylation described above in that the charge-transfer colors in Table I are not observed as transients, owing to the preferential complexation of OsO_4 with pyridine as described in eq 8. Accordingly, this PROMOTED THERMAL or PT osmylation is to be distinguished by the enhanced reactivity of the pyridine complex (see eq 8) relative to the free OsO_4 in the DT osmylation. The corresponding increase in the yields of adducts such as **A**, **P**, and **N** within a shorter span of reaction times is apparent from the comparison of the results of DT and PT osmylations in Tables III and IV, respectively.

IV. Charge-Transfer Osmylation of Benzene, Naphthalene, and Anthracene. The various charge-transfer colors in Table I for the different arene complexes with OsO_4 were persistent for days. However when the colored solutions were deliberately exposed to visible light with energy sufficient to excite only the charge-transfer band, they always deposited a highly insoluble, dark brown solid reminiscent of the OsO_4 adducts obtained from the direct thermal osmylation of arenes (see Table III). Since this actinic process must have arisen via the electronic excitation of the EDA complex according to eq 4, it is referred to hereafter as CHARGE-TRANSFER or CT osmylation for the individual arenes described below.

Benzene. The exposure of the pale yellow solution of benzene and OsO_4 in *n*-hexane to filtered light with $\lambda > 380$ nm corresponded to the irradiation of the low-energy tail of the CT band (see Figure 1A). Nonetheless, a rapid discharge of color occurred, and a deep brown solid separated from the reaction mixture. Similarly, the bright yellow solution of OsO_4 dissolved in *neat* benzene rapidly became turbid and deposited the same brown powder upon irradiation. The amorphous-looking solid was insoluble in chlorinated hydrocarbons, acetone, and water, but it dissolved rapidly in pyridine to give a deep red-brown solution that yielded red-brown microcrystals of **B** (Table V).[46]

Naphthalene. Irradiation of the dark yellow solution of naphthalene and OsO_4 in *n*-hexane with filtered light immediately led to a dark brown precipitate, which was collected and treated with pyridine to afford the 2:1 adduct N as listed in Table V. For these experiments, the focussed beam from a Hg–Xe lamp was passed through a sharp cutoff filter to ensure that only light at the wavelengths $\lambda > 415$ nm impinged on the photochemical cell. An inspection of Figure 1B shows that such irradiation could excite only the charge-transfer band of the complex [$C_{10}H_8$, OsO_4]. It was thus established that the appearance of the dark brown precipitate was the direct consequence of the population of the CT excited state. The CT osmylation of 1,4-dimethylnaphthalene

(43) Conversion refers to the amount of adduct formed relative to OsO_4 charged. The yield based on OsO_4 consumed is close to quantitative.

(44) For structural information see Griffith et al. in ref 35c.
(45) Clark, R. L.; Behrmann, E. J. *Inorg. Chem.* **1975**, *14*, 1425.
(46) Similar 2:1 adducts were previously derived from the CT osmylation of mesitylene and hexamethylbenzene.[19]

Table IV. Promoted Thermal (PT) Osmylation of Polycyclic Arenes with OsO_4–Pyridine[a]

arene	(M)	solvent[b]	promoter[c]	time (h)	adduct[d]	conv,[e] %
phenanthrene	(0.17)	bz	py-d_5	336	P[f]	86
	(0.41)	py		312	P	75
anthracene	(0.11)	bz	py	48	A	72
anthracene	(0.12)	bz	py-d_5	72	A[f]	83
9-methyl	(0.12)	bz	py-d_5	144	A_m[f,g]	82
9-methoxy	(0.10)	bz	py-d_5	96	A_o[f,h]	83
9-bromo	(0.057)	bz	py-d_5	240	A_b[f,i]	78
9-cyano	(0.071)	bz	py-d_5	288	A_c[f,j]	78
9-nitro	(0.059)	bz	py-d_5	288	A_n[f,k]	71
9,10-dimethyl	(0.083)	bz	py-d_5	24	A_{m2}[f,m]	68
9,10-dibromo	(0.092)	bz	py-d_5	336	A_{b2}[f,n]	72
naphthalene	(0.10)	bz	py	720	N	29
naphthalene	(0.066)	bz	py-d_5	1680	N[f]	52
1,4-dimethyl	(0.11)	bz	py-d_5	336	N_{m2}[f,p]	20
	(0.18)	py		168	N_{m2}[p]	73
1-methoxy	(0.17)	bz	py-d_5	888	N_o[f,q]	73
2,6-dimethoxy	(0.11)	bz	py-d_5	888	N_{o2}[f,r]	61

[a] In 5 mL of solvent at 25 °C. [b] bz = benzene, py = pyridine. [c] 2 equiv relative to OsO_4. [d] For structural assignment of the single isomer, see Experimental Section. [e] Conversion based on arene charged. [f] With py-d_5 ligands. [g] 9-methyl-A. [h] 9-methoxy-A. [i] 9-bromo-A. [j] 9-cyano-A. [k] 9-nitro-A. [m] 9,10-dimethyl-A. [n] 9,10-dibromo-A. [p] 1,4-dimethyl-N. [q] 1-methoxy-N. [r] 2,6-dimethoxy-N.

under the same photochemical conditions resulted in the 2:1 adduct, namely

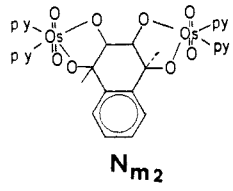

N_{m2}

as described in the Experimental Section.

Phenanthrene. The purple solution of phenanthrene and OsO_4 in carbon tetrachloride was irradiated at $\lambda > 380$ nm to ensure that only the CT absorption band was excited (see Table I). The dark brown precipitate after treatment with pyridine yielded red-brown crystals of a single isomer of the 1:1 adduct **P** (vide supra). Comparative results in Tables V and III indicated that a possible competition from the DT osmylation was much too slow for any significant contribution to the formation of **P** under these photochemical conditions.

Anthracene. Of the arenes examined in this study, anthracene was unique in that it afforded two entirely different types of products upon the photoexcitation of the EDA complex [$C_{14}H_{10}$, OsO_4] in dichloromethane and hexane, despite only minor solvent effects on the charge-transfer bands in Table I. Irradiation of the purple solution of anthracene and OsO_4 in dichloromethane at $\lambda > 480$ nm yielded the 2:1 adduct **A** together with its syn isomer (vide supra) as the sole products in Table VI. On the other hand, irradiation of the same purple-colored solution but in *n*-hexane under otherwise identical conditions led to a small (but discrete) amount of a refractory black precipitate, the analysis of which accorded with the polymeric formulation $(OsO_2)_x$ as described in the Experimental Section. Workup of the hexane solution yielded anthraquinone as the major product contaminated with only traces (<1%) of the 2:1 adduct **A**. Interestingly, even higher yields of anthraquinone were obtained from 9-bromo-, 9-nitro-, and 9,10-dibromoanthracene when the CT osmylation was carried out in *n*-hexane. Such an accompanying loss of the electronegative substituents (X = Br, NO_2) probably occurred via osmylation at the meso (9,10-) positions followed by oxidative decomposition of the unstable adduct with a stoichiometry such as[47]

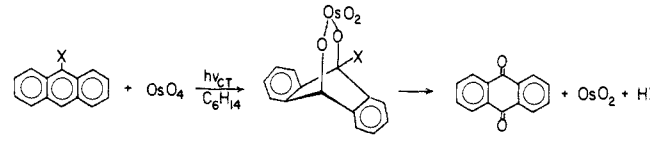

(10)

Table V. Charge-Transfer (CT) Osmylation of Benzene, Naphthalene, and Phenanthrene with OsO_4[a]

arene	(mmol)	OsO_4 (mmol)	solvent	time (h)	λ_{irrad}[b] (nm)	adduct	conv (10^5 mmol)
benzene[c]		0.63	C_6H_6	3.5	380	B	3.2
naphthalene	(0.78)	0.59	C_6H_{14}	8.5	415	N[d]	2.3
naphthalene	(0.61)	0.90	CH_2Cl_2	7.5	415	N[e]	0.5
1,4-dimethylnaphthalene	(0.68)	0.57	C_6H_{14}	4.3	425	N_{m2}	5.0
2,6-dimethoxynaphthalene	(0.36)	0.76	CH_2Cl_2	10.0	415	<0.1	<0.1
	(0.072)	0.60	C_6H_{14}	18.5	425	0	*f*
1-methoxynaphthalene	(0.28)	0.57	CH_2Cl_2	12.3	425	<0.1	*g*
	(0.28)	0.57	C_6H_{14}	12.3	425	0	*h*
phenanthrene	(0.83)	0.98	CCl_4	8.8	380	P	10

[a] In 3 mL of solvent at 25 °C. [b] Low limit of cutoff filter. [c] Neat. [d] As 75/25 mixture of anti/syn N isomers. [e] As 57/43 mixture of anti/syn isomers. [f] 7×10^{-6} mol OsO_2 observed. [g] 1×10^{-6} mol OsO_2. [h] 9×10^{-6} mol OsO_2.

Table VI. Solvent Effect on the CT Osmylation of Anthracenes with OsO_4[a]

X-anthracene	(mmol)	OsO_4 (mmol)	solvent	time (h)	adduct (10^5 mmol)	anthraquinone (10^5 mmol)	OsO_2 (10^5 mmol)
unsubstituted	(0.34)	1.2	CH_2Cl_2	5.5	5.0[b]	0	0
unsubstituted	(0.12)	1.2	CH_2Cl_2	17.5	7.0[c]	0	0
unsubstituted	(0.12)	1.0	C_6H_{14}	17.5	<0.1[d]	0.2	0.4
9-bromo	(0.12)	0.36	C_6H_{14}	4.8	<0.1[d]	1.2	2.9
9,10-dibromo	(0.11)	1.2	C_6H_{14}	3.3	<0.1[d]	3.3	5.3
9,10-dibromo	(0.12)	0.36	CH_2Cl_2	17.5	<0.1[d]	<0.5	0
9-nitro	(0.13)	0.99	C_6H_{14}	18.	<0.1[d]	1.5	1.9
9-cyano	(0.025)	0.98	C_6H_{14}	5.5	<0.1[d]	<0.1	0.4
9-methyl	(0.32)	0.64	C_6H_{14}	12.3	1.5[e]	0	0
9,10-dimethyl	(0.32)	0.64	C_6H_{14}	12.3	0.8[f]	0	0
9,10-dimethyl	(0.32)	0.64	CH_2Cl_2	12.3	1.0[g]	0	0

[a] In 3 mL of solvent at 25 °C with $\lambda > 480$ nm unless indicated otherwise. [b] As a 50/50 anti/syn mixture. [c] As a 42/58 anti/syn mixture. [d] Traces. [e] 50/50 anti/syn. [f] 85/15 anti/syn. [g] 56/44 anti/syn.

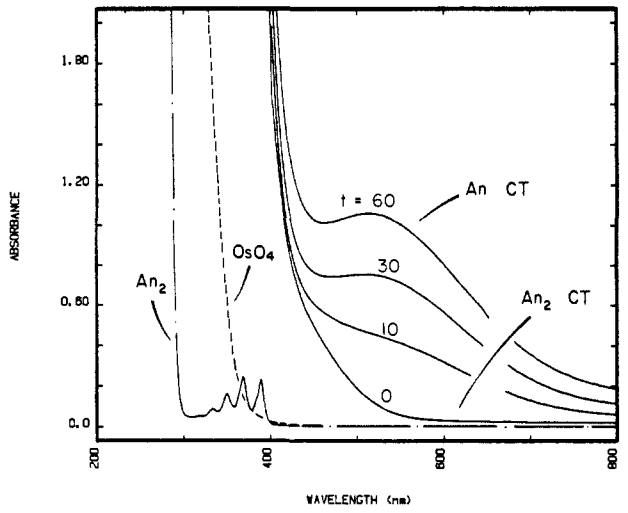

Figure 5. Charge-transfer cycloreversion of 5×10^{-6} M di-9-methylanthracene with 7×10^{-4} M OsO_4 in dichloromethane showing the change of the CT band of dimer at time $t = 0$ to that of the EDA complex of the monomeric [MeAn, OsO_4] at $t = 10$, 30, and 60 min following irradiation at $\lambda > 415$ nm. The absorption spectra of dianthracene (—·—) and OsO_4 (---) at the same concentrations are also shown for comparison.

It is noteworthy that neither 9-cyano-, 9-methyl-, nor 9,10-dimethylanthracene yielded anthraquinone when the CT osmylations were carried out in hexane. The oxidation product that accompanied the small amount of OsO_2 from 9-cyanoanthracene in hexane was not identified. Only a 2:1 adduct (and no reduced OsO_2) was detected from both 9-methyl- and 9,10-dimethylanthracene, as listed in Table VI.

Dianthracene. As the head-to-tail 9,10-dimer, dianthracene is optically transparent below 300 nm owing to the presence of only benzenoid chromophores. Thus the solution of osmium tetroxide admixed with dianthracene in dichloromethane afforded immediately the yellow color characteristic of the EDA complex of benzenoid aromatics. However the irradiation of this solution at $\lambda > 410$ nm using a sharp cutoff filter differed dramatically from that observed with benzene (vide supra). First, the yellow solution turned purple, and the change in the absorption spectrum clearly identified the growth of a new band with $\lambda_{max} = 510$ nm, which was diagnostic of the [anthracene, OsO_4] complex described in Table I. The series of color changes are illustrated in Figure 5 for the 9-methyl analogue owing to its slightly enhanced solubility. Second, only small amounts of OsO_4 adducts to anthracene were formed under these conditions, as indicated by the trace observation of dark brown precipitate (vide supra). Indeed the quantitative analysis of the solution by gas chromatography (following the removal of OsO_4) indicated cycloreversion according to the stoichiometry shown in eq 11. Since this fragmentation arises directly via photoexcitation of the EDA complex of dianthracene with OsO_4, it is designated as *charge-transfer cycloreversion.*

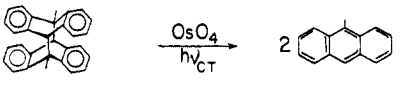

(11)

Quantum yields for the CT osmylation of arenes and the CT cycloreversion of dianthracene in Table VII were measured with Reinecke salt actinometry[48] by following the changes in the arene concentrations spectrophotometrically. The same result (entry 2) was obtained when the course of CT osmylation was followed by the decrease in the absorbance of the charge-transfer band.

Table VII. Quantum Yields for the Charge-Transfer Osmylation of Arenes and CT Cycloreversion of Dianthracene[a]

arene	OsO_4 (mmol)	OsO_4 (mmol)	solvent	$10^2\Phi_p$
anthracene	(0.013)	5.75	C_6H_{14}	0.5 (1), 0.8 (2)[b]
	(0.036)	4.18	CH_2Cl_2	0.9 (1)
naphthalene	(0.084)	2.16	C_6H_{14}	1.2 (1)
	(0.11)	2.23	CH_2Cl_2	0.3 (1)
9,10-dibromoanthracene	(0.0066)	5.21	C_6H_{14}	3.0 (3)
9-methylanthracene dimer	(0.0096)	4.05	CH_2Cl_2	5.0 (5)[c]

[a] In 3 mL solvent at 25 °C with Reinecke salt actinometry by arene disappearance. [b] By change in CT absorbance. [c] By appearance of arene.

V. Time-Resolved Spectra of the Reactive Intermediates in Charge-Transfer Osmylation. In order to identify the reactive intermediates in the charge-transfer excitation of arene–OsO_4 complexes, we examined the time-resolved spectra immediately following the application of a 30-ps pulse consisting of the second harmonic at 532 nm of a mode-locked Nd:YAG laser. The wavelength of this excitation source corresponded to the maxima (or near maxima) of the charge-transfer absorption bands of the series of anthracene complexes with osmium tetroxide illustrated in Figure 1C. Accordingly, the time-resolved spectra obtained from the anthracene–OsO_4 system related directly to the CT osmylation in Table VI since there was no ambiguity about either the adventitious local excitation[27] of complexed (or uncomplexed) chromophores or the photogeneration of intermediates that did not arise from the photoexcitation of the EDA complex. Indeed, intense absorptions were observed in the visible region between 700–800 nm from the excitation of the anthracene–OsO_4 complexes, as shown in Figure 6. The time-resolved absorption spectra from anthracene and 9-cyanoanthracene in Figure 6 (parts A and B, respectively) represented the composite (normalized) of six spectra taken in the time interval between 20 and 50 ps following the application of the 532-nm laser pulse. Comparison with the steady-state absorption spectra of the corresponding anthracene cation radicals (see insets) generated by the spectroelectrochemical technique,[49] thus established the identity of the charge-transfer transient. Similar time-resolved spectra of arene cation radicals were obtained from the naphthalene EDA complexes despite the excitation of only the low-energy tails of the CT bands in Figure 1B with the 532-nm laser pulse. The slight red-shift in λ_{max} of the cation radical from the electron-rich 1,4-dimethylnaphthalene (IP 7.78 eV) relative to that of naphthalene (IP 8.12 eV) is shown in Figure 7. For comparison, the time-resolved spectrum of the cation radical from 9,10-dibromoanthracene (IP 7.54 eV) is also included in Figure 7C.

VI. Temporal Evolution of Arene Cation Radicals during Charge-Transfer Osmylation. The transient absorption spectra in Figures 6 and 7 identify the arene cation radical ($Ar^{\bullet+}$) as the initial reactive intermediate in CT osmylation. The evolution of the anthracene cation radical was followed by measuring the absorbance change at $\lambda_{max} = 742$ nm (see Figure 6A) upon the charge-transfer excitation of the EDA complex with a single laser shot of ~10 mJ. The time evolution of the absorbance shown in Figure 8 (left) includes the initial onset for ~20 ps owing to the rise time of the 30-ps (fwhm) laser pulse. The first-order plot of the decay portion is shown in the inset to the figure. The latter was more clearly defined for the 9-cyanoanthracene cation radical in Figure 8 (right).

Decay curves similar to those shown in Figure 8 were also observed for the disappearances of the cation radicals derived from the other arene–OsO_4 complexes listed in Table VIII. In each

(47) (a) The formation of anthraquinone may of course be stepwise and involve the attachment of only one and not two oxygen(s) of OsO_4 to the anthracene. (b) The fates of the cleaved bromo and nitro substituents were not traced. (c) Although isotopic tracers were not employed, osmium tetroxide is the only source of oxygen in the system.

(48) Wegner, E. E.; Adamson, A. W. *J. Am. Chem. Soc.* **1966**, *88*, 394.

(49) (a) Masnovi, J. M.; Kochi, J. K.; Hilinski, E. F.; Rentzepis, P. M. *J. Am. Chem. Soc.* **1986**, *108*, 1126. (b) With some other arenes, we observed spectral shifts between the time-resolved ps and steady-state spectra of the cation radicals (Sankararaman, S., unpublished results), and they will be elaborated later.

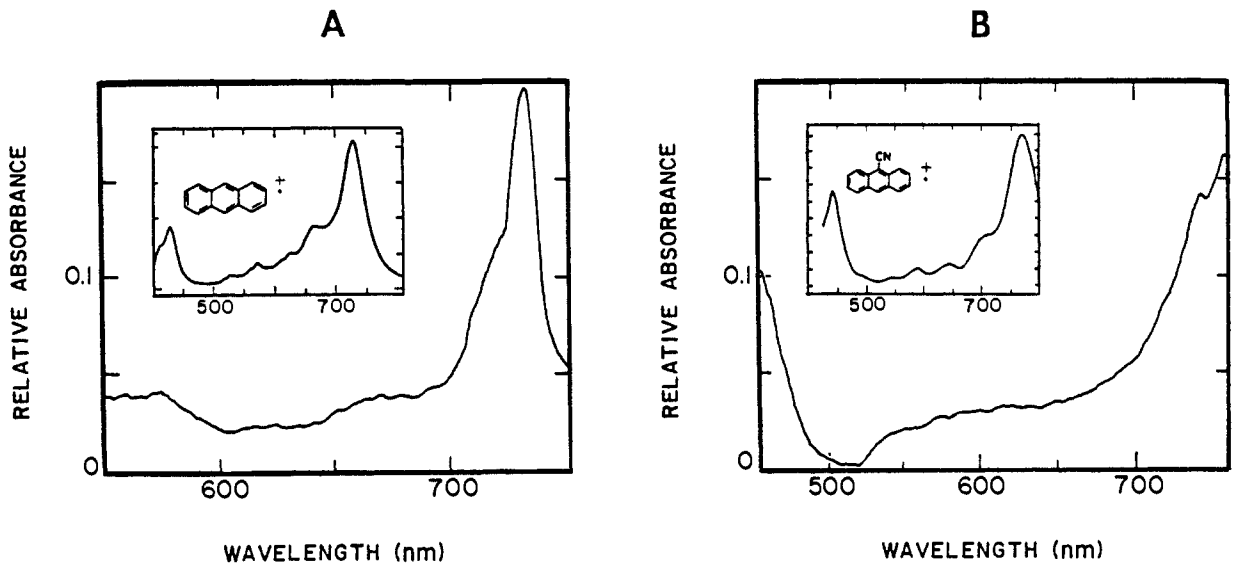

Figure 6. Transient absorption spectrum of the cation radical from (A) anthracene and (B) 9-cyanoanthracene in CH_2Cl_2 at ~35 ps following the 532-nm CT excitation of the OsO_4 complex with 30-ps (fwhm) laser pulse. The insets are the steady-state spectra obtained by spectroelectrochemical generation in ref 49.

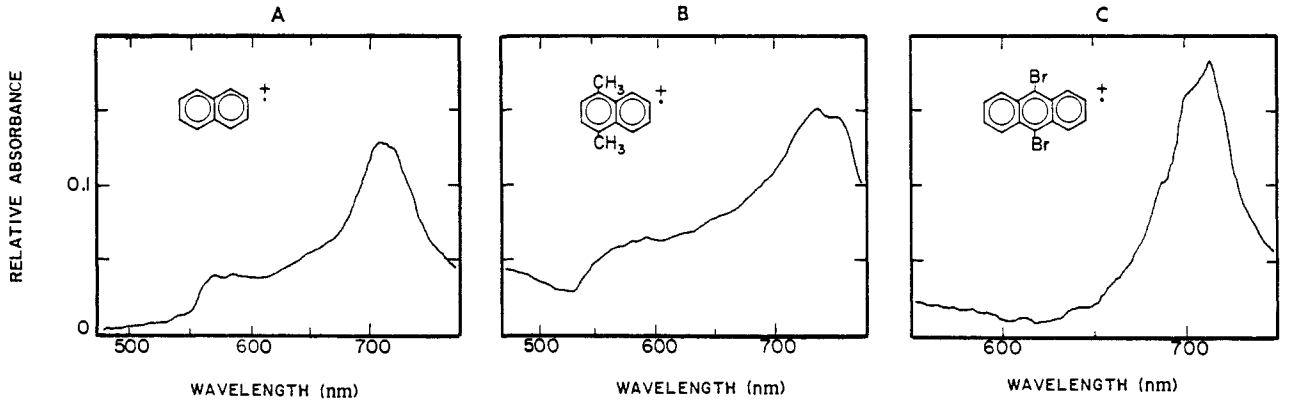

Figure 7. Time-resolved absorption spectra of (A) naphthalene, (B) 1,4-dimethylnaphthalene, and (C) 9,10-dibromoanthracene cation radicals generated in CH_2Cl_2 during CT osmylation as in Figure 6.

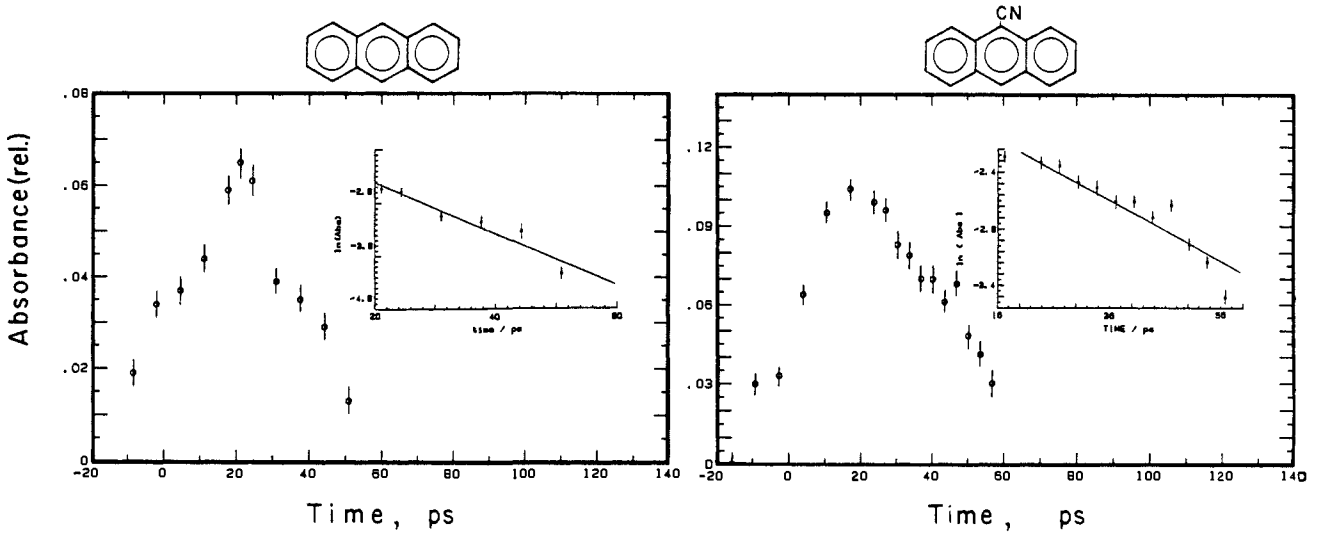

Figure 8. Typical appearance and decay of the CT transient from (left) anthracene and (right) 9-cyanoanthracene in dichloromethane by following the change of the absorbance at λ_{max} = 742 and 758 nm, respectively. The inset shows the first-order plots of the absorbance decay subsequent to the maximum at ~20 ps.

case, the concentrations of the arene (usually of limited solubility) and osmium tetroxide were first optimized for maximum absorbance of the CT band. This procedure allowed the highest concentration to be obtained of the arene cation radical, the decays of which were all uniformly treated as first-order processes.[50] The magnitudes of the rate constant k_1 in Table VIII were applicable to the complete disappearance of $Ar^{\bullet+}$, as indicated by the return

(50) The choice was dictated by the minimal role of diffusional processes on this time scale. For a discussion see ref 20 and 49.

Table VIII. First-Order Decay of Arene Cation Radicals during CT Osmylation[a]

arene	(M)	OsO_4 (M)	A_{532}[b]	λ_{Ar^+}[c] (nm)	k_1[d] (10^{-10} s^{-1})
anthracene	(0.11)	0.10	1.58	742	4.9
	(0.13)	0.16	2.9[e]	750	5.3
9-bromo	(0.04)	0.17	1.08	720	5.6
	(0.03)	0.28	1.74	697[f]	1.4
9-cyano	(0.05)	0.25	0.83	758	2.8
9-nitro	(0.05)	0.25	0.63	750	4.9
9,10-dibromo	(0.03)	0.58	1.97	721	2.8
phenanthrene	(0.35)	0.12	1.30	725	4.6
naphthalene	(0.54)	0.26	1.7	710	4.5
1,4-dimethyl	(0.33)	0.10	2.0	740	2.0

[a] In CH_2Cl_2 at 25 °C, unless indicated otherwise. [b] Absorbance at the excitation wavelength. [c] Absorption maximum of the arene cation radical. [d] Data treated as a first-order decay. [e] Two independent measurements. [f] In hexane solution.

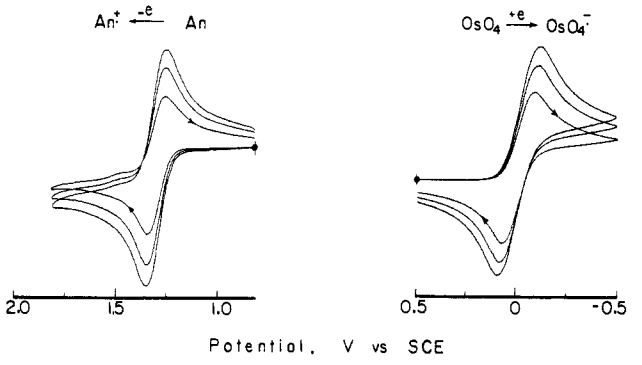

Figure 9. Cyclic voltammograms of (left) the initial positive scan of 5 × 10^{-3} M of anthracene and (right) initial negative scan of 5 × 10^{-3} M osmium tetroxide in dichloromethane containing 0.1 M TBAH at v = 200, 400, and 600 mV s^{-1}.

of the cation-radical absorbances to the base line. No other transient absorptions were observed in this spectral region, even when the time-resolved spectroscopy was carried out on the extended ns and μs time scales.[51]

VIII. Electrochemical Formation and Spectral Identification of Arene Cation Radicals and the Osmium(VII) Anion Radical. The identification of the CT ion pair in Scheme II requires independent verification as the separate arene cation radical and osmium(VII) anion radical. The anthracenes represent viable donors for electrochemical methods of electron detachment since the cation radical is persistent on the cyclic voltammetric time scale. Thus the cyclic voltammogram in Figure 9 (left) shows the initial *positive* scan of a 5 × 10^{-3} M solution of anthracene in dichloromethane containing 0.1 M tetra-*n*-butylammonium hexafluorophosphate (TBAH). The reversible redox couple

$$An \rightleftharpoons An^+ + e \qquad \text{at } E_0 = 1.30 \text{ V vs SCE}$$

for anthracene in dichloromethane is indicated by the ratio of anodic and cathodic peak currents $i_p^a/i_p^c = 1.1$.[52] The transient anodic spectroelectrochemistry of this anthracene solution at a platinum microgrid electrode produced the absorption spectrum of the cation radical shown in the inset of Figure 6 (left). Analogously the cyclic voltammogram in Figure 9 (right) shows the initial *negative* scan of a 5 × 10^{-3} M solution of osmium tetroxide also in dichloromethane containing 0.1 M TBAH. The reversible redox couple

$$OsO_4 + e \rightleftharpoons OsO_4^- \qquad \text{at } E_0 = -0.06 \text{ V vs SCE}$$

(51) Compare: Sankararaman, S.; Haney, W. A.; Kochi, J. K. *J. Am. Chem. Soc.* **1987**, *109*, 5235, 7824.

(52) Bard, A. J.; Faulkner, L. R. *Electrochemical Methods*; Wiley: New York, 1980. See also footnote 6 in ref 21 and Hammerich and Parker (Hammerich, O.; Parker, V. D. *J. Am. Chem. Soc.* **1974**, *96*, 4289).

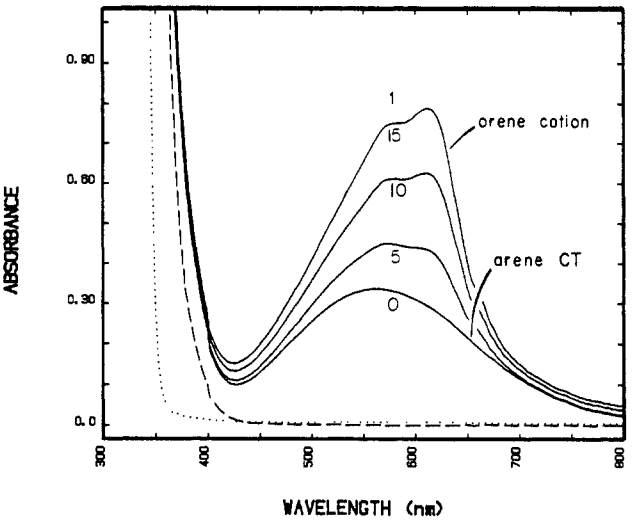

Figure 10. Spontaneous formation of arene cations from the EDA complex of 2.5 × 10^{-2} M 1,4-dimethoxynaphthalene and 5 × 10^{-2} M OsO_4 in hexane. The CT band at t = 0 is followed by the growth of the cation absorbance at t = 5, 10, and 15 min. The spectra of the separate arene (···) and OsO_4 (---) are at the same concentrations.

in dichloromethane is indicated by the ratio $i_p^c/i_p^a = 1.0$. The spectroelectrochemistry of osmium tetroxide (λ_{max} = 305 nm, ϵ = 900 M^{-1} cm^{-1} in dichloromethane) showed an absorbance increase in the region of ~300 nm, but a distinctive band for OsO_4^- could not be discerned.[53]

Discussion

Osmium tetroxide is a versatile electron acceptor that is capable of forming a wide range of electron donor–acceptor (EDA) complexes with alkene and arene donors (eq 1). In this study we have successfully established how the [Ar, OsO_4] complexes are involved as precursors in the oxidative addition of osmium tetroxide to various arenes by the three independent procedures herein designated as direct thermal (DT), promoted thermal (PT), and charge-transfer (CT) osmylation. For example, the anthracenes react rather slowly with osmium tetroxide via the EDA complex to effect DT osmylation in nonpolar solvents and afford 2:1 adducts that are then converted to the more tractable pyridine derivatives such as **A** (see Figure 4). Alternatively, the same ternary product **A** is directly formed at a significantly *enhanced* rate by the PT osmylation of anthracene with a mixture of OsO_4 and pyridine (eq 8). Finally, the OsO_4 adduct to anthracene is instantly produced by CT osmylation involving actinic excitation of the [Ar, OsO_4] precursor complex. As such, the three procedures represent different activation mechanisms for arene oxidation. Thus DT and PT osmylations are adiabatic processes in which the transition states are attained via the collapse of an arene donor with the OsO_4 and the base-coordinated OsO_4(py) electrophile, respectively. On the other hand, CT osmylation is a nonadiabatic process resulting from the vertical excitation of the [Ar, OsO_4] complex. For the latter, time-resolved picosecond spectroscopy can define the relevant photophysical and photochemical events associated with the charge-transfer excitation of an arene EDA complex in eq 4, as we have previously shown with arene complexes involving other electron acceptors.[20,49] Accordingly let us first establish the mechanism of CT osmylation and then enquire as to how it can be related to either DT or PT osmylation or to both. Before

(53) (a) We judge that the electronic absorption spectrum of OsO_4^- is similar to that of OsO_4 [Wells, E. J.; Jordan, A. D.; Alderdice, D. S.; Ross, I. G. *Austr. J. Chem.* **1967**, *20*, 2315] with an absorption band at ~300 nm, since by comparison the absorption spectra of the related oxoruthenium complexes RuO_4 and RuO_4^- are quite similar, both showing distinctive bands with λ_{max} = 385 nm [Seddon, E. A.; Seddon, K. R. *Chemistry of Ruthenium*; Elsevier: Amsterdam, 1984, p 58.] (b) We thank a referee for kindly pointing out a recent report of the isolation and characterization of the perosmate salt $Ph_4As^+OsO_4^-$ by Bilger et al. (Bilger, E.; Pebler, J.; Weber, R.; Dehnicke, K. *Z. Naturforsch.* **1984**, *39B*, 259).

Scheme I

$$Ar + OsO_4 \xrightarrow{slow} ArOsO_4 \quad (12)$$

$$ArOsO_4 + OsO_4 \xrightarrow{fast} Ar(OsO_4)_2 \quad (13a)$$

$$xAr(OsO_4)_2 \xrightarrow{fast} [Ar(OsO_4)_2]_x \quad (13b)$$

Scheme II[a]

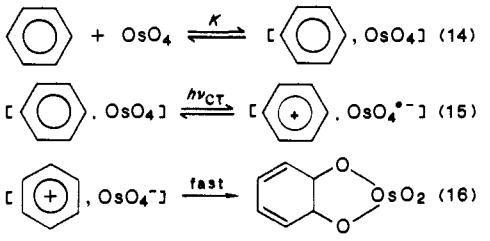

[a] Where the brackets denote solvent-caged pairs.

proceeding however it is important to emphasize that the DT, PT, and CT osmylations all share in common the formation of the 1:1 osmium(VI) cycloadduct $ArOsO_4$ in the initial rate-limiting step, since the concomitant loss of aromaticity produces a reactive alicyclic diene that is highly susceptible to further osmylation.[5] The universal adherence to the 2:1 adduct $Ar(OsO_4)_2$ (except phenanthrene), irrespective of the molar ratios of arene/OsO_4 and the particular procedure employed, accords with the rapid addition of a second mole of OsO_4 in DT, PT, and CT osmylations. Furthermore the ubiquitous precipitation of the dark brown solid in DT and CT osmylations arises from the ready formation of polymeric structures, e.g.

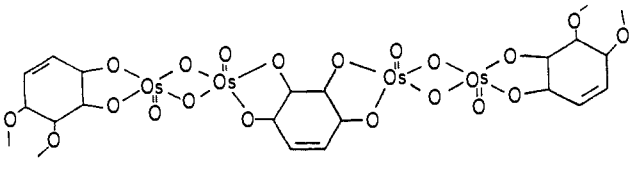

that result from the mutual association of the coordinatively unsaturated osmium(VI) centers in $Ar(OsO_4)_2$.[54] The general sequence of common intermediates depicted below allows us to now focus on the formation of a single intermediate $ArOsO_4$ (eq 12) in order to delineate the unifying activation processes for DT, PT, and CT osmylations.

I. Mechanism of the Charge-Transfer Osmylation of Arenes. The direct observation of the reactive intermediates by the use of time-resolved picosecond spectroscopy (Figures 6 and 7) and fast kinetics (Figure 8) enables the course of CT osmylation to be charted in some detail. We proceed in the analysis from the mechanistic context involving the evolution and metamorphosis of the CT ion pair, as summarized in Scheme II for the critical initial step (eq 12) to form the 1:1 adduct to a benzene donor.

All the experimental observations on CT osmylation indeed coincide with the mechanistic formulation in Scheme II. Thus the exposure of arene to osmium tetroxide leads immediately to new absorption bands (Figure 1) that are readily associated with the formation of the EDA complex in eq 14. These binary complexes are always present in low steady-state concentrations owing to the limited magnitudes of K determined by the Benesi–Hildebrand method (Table II). The complexes are so weak that every attempt at isolation, including the freezing of various mixtures of OsO_4 in neat aromatic donors, merely led to phase separation.[10,55] The absorption bands in Table I are thus properly ascribed to contact charge transfer, as formulated by Orgel and Mulliken,[59] who predicted the CT absorption bands in these EDA complexes to be associated with the electronic excitation to the ion-pair state (eq 15). As such the time-resolved spectra in Figures 6 and 7 identify the formation of arene cation radicals to occur within the rise time of the 30-ps laser pulse. [The accompanying presence of the perosmate(VII) (OsO_4^-) counteranion is obscured by the arene absorptions.[60]] We thus conclude that the electron transfer from the arene donor to the OsO_4 acceptor in the EDA complex in eq 15 effectively occurs with the absorption of the excitation photon ($h\nu_{CT}$), in accord with Mulliken's theory.[27] Furthermore the appearance at <30 ps demands that Ar^+ and OsO_4^- are born as an intimate ion pair with a mean separation essentially that of the precursor complex [Ar, OsO_4] since this time scale obviates significant competition from diffusional processes.[20,49] The seminal role of the ion pair [Ar^+, OsO_4^-] as the obligatory intermediate from the photoexcitation of the EDA complex must be included in any mechanistic formulation of CT osmylation by taking particular cognizance of how it decays.

The spontaneous collapse of the CT ion pair in eq 16 represents the most direct pathway to arene cycloaddition[61]—the measured half-life of $\tau \cong 35$ ps for the disappearance of the anthracene cation radicals in Figure 9 largely precluding diffusive separation of such ion pairs. However the magnitudes of the product quantum yield $\Phi_p \sim 10^{-2}$ in Table VII indicate that the primary route for ion-pair decay is the back electron transfer (k_{ET}) as the reverse step of eq 15. Such an energy-wasting process with an estimated rate constant of $k_{ET} \sim 10^{11}$ s^{-1} derives from a highly exergonic driving force that is estimated to be $\Delta G \cong -30$ kcal mol^{-1} based solely on the standard redox potentials in Figure 9 of $E^0 = +1.30$ and -0.06 V for anthracene and the perosmate (VII) anion, respectively.[62] A similar estimate of the rate of back electron transfer is obtained from the OsO_4-induced cycloreversion of dianthracene (An_2) by the irradiation of the CT absorption band (Figure 5) of the precursor complex, i.e.

(54) For a summary, see: Griffith, W. P. in ref 37 and Gulliver, D. J.; Levason, W. in ref 41c.

(55) (a) Nonetheless we made many extensive but fruitless efforts to isolate these as 1:1 complexes, analogous to our recent successful efforts with the similarly weak tetrabromomethane complexes.[56] Indeed both electron acceptors exhibit a tetrahedral configuration about the central core atom. For arene donors with tetrabromomethane, X-ray crystallography has established the HOMO–LUMO interaction to involve a delocalized bromine "bond".[57] An analogous structure for the OsO_4 complex would find the oxygen atom of the osmyl moiety lying directly on the 6-fold symmetry axis as opposed to a π–π interaction involving the oxo–osmium bond.[58] (b) For the tetrahedral structure of OsO_4, see: Krebs, B.; Hasse, K. D. *Acta Crystallogr.* **1976**, *B32*, 1354 and Seip, H. M.; Stolevik, R. *Acta Chem. Scand.* **1966**, *20*, 385.

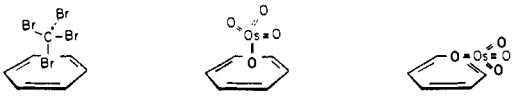

(56) (a) Blackstock, S. C.; Kochi, J. K. *J. Am. Chem. Soc.* **1987**, *109*, 2484. Blackstock, S. C.; Lorand, J. P.; Kochi, J. K. *J. Org. Chem.* **1987**, *52*, 1451. (b) Note however the weak complexes isolated were derived from rather localized, strong σ-donors rather than the delocalized, weaker π-donors typical of arenes.

(57) Streiter, F. J.; Templeton, D. H. *J. Chem. Phys.* **1962**, *37*, 161.

(58) Although the arene donors are presented as η^6-ligands, it is also possible for them to act as η^2-ligands in CT photochemistry. See: Lau, W.; Kochi, J. K. *J. Org. Chem.* **1986**, *51*, 1801.

(59) Orgel, L. E.; Mulliken, R. S. *J. Am. Chem. Soc.* **1957**, *79*, 4839.

(60) (a) The visible absorption spectrum of $Ph_4As^+OsO_4^-$[53b] shows a strong band with $\lambda_{max} = 296$ nm and a very broad, weak band with $\lambda_{max} \sim 500$ nm extending beyond 800 nm in dichloromethane. (b) The absorption spectrum of the related perruthenate(VII) RuO_4^- has been reported by Connick et al. (Connick, R. E.; Hurley, C. R. *J. Am. Chem. Soc.* **1952**, *74*, 5012). See, also: Silverman, M. D.; Levy, H. R. *J. Am. Chem. Soc.* **1954**, *76*, 3317, 3319.

(61) (a) The process may be either stepwise (one oxo ligand) or concerted (both oxo ligands). For the cycloaddition of a related ion pair, see: Takahashi, Y.; Kochi, J. K. *Chem. Ber.* **1988**, *121*, 253. (b) It is also possible but unlikely to occur by back electron transfer followed by the recombination of the vibrationally "hot" reactant pair.

(62) The sizeable electrostatic energy inherent in tight ion pairs is neglected. See Fukuzumi, S.; Kochi, J. K. *Bull. Chem. Soc. Jpn.* **1983**, *56*, 969. (b) By comparison with RuO_4 (vide supra), the reorganization energy for $OsO_4 \rightarrow OsO_4^{\bullet-}$ is likely to be small. Thus the rate of back electron transfer of the ion pair in eq 15 will be fast. See: Klingler, R. J.; Kochi, J. K. *J. Am. Chem. Soc.* **1981**, *103*, 5839.

Scheme III

$$[An_2, OsO_4] \overset{h\nu_{CT}}{\rightleftharpoons} [An_2^+, OsO_4^-] \quad (17)$$

$$[An_2^+, OsO_4^-] \xrightarrow{fast} [An, An^+, OsO_4^-], \text{ etc.} \quad (18)$$

The high quantum yield of $\Phi_p = 0.05$ for the cycloreversion indicates that the rate constant k_{ET} for the back electron transfer as the reverse step of eq 17 is $\sim 10^{10}$ s^{-1} since the half-life of the dianthracene cation radical (eq 18) was previously estimated to be $\sim 10^{-8}$ s.[63] However more relevant to this issue here is an estimated first-order rate constant for cycloaddition of $k_c = 10^9$ s^{-1} for the ion-pair collapse to the arene cycloadduct in Scheme II.[64] Such a relatively large rate constant also points to a highly exergonic (bond-making) process for the cycloaddition in eq 16.[61] Let us therefore consider the selectivity in adduct formation from various polynuclear arenes in which the initial addition of OsO_4 is possible at several sites. The regiospecificity observed in the CT osmylation of phenanthrene and 1,4-dimethylnaphthalene to produce only one isomeric adduct **P** and $\mathbf{N}_{m2}$, respectively, accords with the reactive site centered on the arene HOMO.[65] However in the extended polynuclear anthracenes, the separation of the HOMO and subjacent SHOMO (i.e., HOMO-1) is not so well delineated,[66] and the regiospecificity is strikingly modulated by solvent polarity (Table VI). Ion-pair annihilation is known to occur with the greatest ease in highly nonpolar alkanes.[67] Accordingly in *n*-hexane as solvent, the immediate collapse of the first-formed ion pair centered at the anthracene HOMO is expected to occur at the meso (9,10-) positions. Such an ion-pair collapse would produce anthraquinone in a manner similar to that presented in eq 10.[47] On the other hand, the formation of *only* adduct **A** from the initial addition of OsO_4 to the terminal ring represents a very unusual regiospecificity insofar as other addition (and substitution) reactions of anthracene are concerned.[68-70] We tentatively suggest that the initially formed HOMO ion pair (HIP) has time to relax in the more polar dichloromethane medium to the isomeric SHOMO ion pair (SIP) that rapidly leads to adduct **A**.[71] As speculative as this proposal is, it receives a modicum of credibility

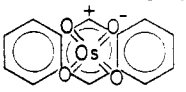
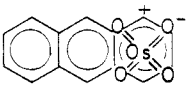

from the observation of adducts related to **A** from the CT osmylation of both 9-methyl- and 9,10-dimethylanthracene in *hexane* (see Table VI). The enhanced stability of the cation radicals from these relatively electron-rich anthracenes will optimize the opportunity to convert the HIP to the more reactive SIP even in the nonpolar hexane medium,[72] particularly if the collapse of the former were reversible.[73] Be that as it may, the postulation of at least two types of primary ion pairs by solvent variation is amenable to experimental verification by time-resolved spectroscopy such as that shown in Figures 6 and 7, particularly at the subpicosecond time scale.[74]

II. Electron-Transfer Mechanism for the Direct Thermal Osmylation of Arenes. Let us now direct our attention to the DT osmylation of arenes in the light of the mechanism established for CT osmylation according to Scheme II. Although the rates of the DT osmylation of most arenes are too slow to measure accurately, the qualitative results in Table III provide a meaningful measure of arene reactivity sufficient for our purposes here. Thus the trend in rates, anthracene > phenanthrene > 1,4-dimethylnaphthalene > naphthalene ≫ benzene, follows the order of increasing ionization potentials of the arenes (Table I). Most importantly, the detailed comparison of the entries in Table III with those in Tables V and VI show that the various types of arenes form the *same adducts* in DT and CT osmylation. For example, phenanthrene affords the single 1:1 adduct **P** by both processes. Moreover naphthalene yields the 2:1 adduct **N** as essentially the same mixture of anti and syn adducts in DT and CT osmylations. The regiospecificity in OsO_4 addition to unsymmetrical arenes such as 1,4-dimethylnaphthalene also proceeds in the same way at the more electron-rich aromatic center (see adduct $\mathbf{N}_{m2}$). It is particularly noteworthy that the DT osmylation of anthracene occurs by exclusive addition of the OsO_4 electrophile to the terminal ring to afford the 2:1 adduct **A** in high yields with no evidence for attack at a meso position. Furthermore the ratio of anti/syn isomers in Table III is the same as that formed by CT osmylation (Table VI).

The formation of such identical adducts from all the arenes provides a unique insight into DT osmylation vis à vis CT osmylation. Thus these osmylations represent completely opposite poles of reaction time scales—the ion-pair collapse to the arene adduct (eq 16) in CT osmylation occurring in picoseconds, in contrast to weeks and even months for the passage through the transition state of DT osmylation. According to Hammond's postulate,[75] the rapidity of ion-pair collapse reflects a regiospecificity that is controlled by an exothermic, reactant-like process[76] for CT osmylation. By the same reasoning the opposite endothermic, product-like process would describe DT osmylation. Nonetheless they both yield anthracene adducts at the *unfavorable* terminal ring—in apparent violation of the reactivity/selectivity principle.[77] However this conundrum can be resolved if the transition state for DT osmylation bears a strong kinship to the transient ion pair $[Ar^+, OsO_4^-]$ in CT osmylation. The marked

(63) Masnovi, J. M.; Kochi, J. K. *J. Am. Chem. Soc.* **1985**, *107*, 6781.
(64) Although this rate constant is an order of magnitude slower than that for the diffusive separation of uncharged species, CT ion pairs may be longer-lived (see ref 51a).
(65) Compare Brogli, F.; Heilbronner, E. *Theor. Chim. Acta (Berlin)* **1972**, *26*, 289.
(66) (a) Klasinc, L.; Kovac, B.; Gusten, H. *Pure Appl. Chem.* **1983**, *55*, 289. (b) Clark, P. A.; Brogli, F.; Heilbronner, E. *Helv. Chim. Acta* **1972**, *55*, 1415. (c) Boschi, R.; Clar, E.; Schmidt, W. *J. Chem. Phys.* **1974**, *60*, 4406.
(67) Masnovi, J. M.; Kochi, J. K. *J. Am. Chem. Soc.* **1985**, *107*, 7880.
(68) In various types of electrophilic, nucleophilic, homolytic, carbene, oxidative, [2 + 4] and [4 + 4] cycloadditions, etc. For example, see the attack by the following: (a) Cl_2C: Murray, R. W. *Tetrahedron Lett.* **1960**, 27. (b) HNO_3: Meisenheimer, J.; Connerade, H. *Ann.* **1904**, *330*, 133. (c) Br_2: Austin, B. *J. Chem. Soc.* **1908**, *93*, 1763. (d) $ClSO_3H$: Morley, J. O. *J. Chem. Soc., Perkin Trans. 2* **1976**, 1554. (e) CH_3COCl: Merritt, F. R.; Braun, C. E. *Org. Syn.* **1950**, *30*, 1. (f) $(CH_3CH{=}CH)_2$: Yang, N. C.; Libman, J. *J. Am. Chem. Soc.* **1972**, *94*, 1405. (g) $C_7H_7^-$: Kaupp, G.; Gruber, H. W.; Teufel, E. *Chem. Ber.* **1982**, *115*, 3208. (h) c-C_6H_6/*hν*: Kaupp, G.; Teufel, E. *Chem. Ber.* **1980**, 3669. (i) c-C_6H_8/BuO^-: Pines, H.; Stalick, W. M. *Base-Catalyzed Reactions of Hydrocarbons*; Academic: New York, 1977. (j) MeLi/*hν*: Hixson, S. S. *J. Chem. Soc., Chem. Commun.* **1974**, 574. (k) O_2: Corey, E. J.; Taylor, W. C. *J. Am. Chem. Soc.* **1964**, *86*, 3881. (l) $CH_3SOCH_2^-$: Argabright, P. A.; Hofmann, J. E.; Schriesheim, A. *J. Org. Chem.* **1965**, *30*, 3233.
(69) For significant but not exclusive attack at a terminal ring, see the following: (a) CH_2N_2/CuBr: Muller, E.; Kessler, H. *Ann.* **1966**, *692*, 58. (b) EtO_2CN: Beckwith, A. L. J.; Redmond, J. W. *Austr. J. Chem.* **1966**, *19*, 1859. (c) PhN_2^+/CuCl: Dickerman, S. C.; Vermont, G. B. *J. Am. Chem. Soc.* **1962**, *84*, 4150. (d) $CH_3COCl/AlCl_3$: Bassilios, H. *Bull. Soc. Chim. Belg.* **1966**, *75*, 582. (e) O_3: Bailey, P. S. *Ozonation in Organic Chemistry*; Academic: New York, 1982; Vol II, pp 82ff.
(70) (a) Although the parent anthracene affords the 9,10-endo peroxide with singlet oxygen, it is interesting to note that very high selectivities to the 1,4-endo peroxides are obtained only if strongly electron-donating substituents (Me_2N-, MeO-) are at appropriate positions. [See Rigaudy, J. *Pure Appl. Chem.* **1968**, *16*, 169 and related papers.] An electron-transfer mechanism has been proposed. [See Ericksen, J.; Foote, C. S.; Parker, T. L. *J. Am. Chem. Soc.* **1977**, *99*, 6455 and related papers]. For a review, see: Saito, I.; Matsuura, T. In *Singlet Oxygen*; Wasserman, H. H., Murray, R. W., Eds.; Academic: New York, 1979; p 514ff. (b) Furthermore all other reactions of equilibrated anthracene cation radical proceed at the meso positions. See: Yoshida, K. *Electrooxidation in Organic Chemistry*; Wiley: New York, 1984. Masnovi, J. M.; Kochi, J. K. *J. Org. Chem.* **1985**, *50*, 5245.
(71) Owing to the close similarity of the CT spectra in hexane and dichloromethane in Table I, it is unlikely that HIP and SIP arise from different EDA complexes.
(72) For the increased lifetimes of cation radicals from electron-rich anthracenes in nonpolar solvents such as hexane, see discussion in ref 63.
(73) The stepwise collapse of the ion pair[61] could provide the time for reversibility.
(74) For example, for the spectral differences between "tight" and "loose" ion pairs, see Simon, J. D.; Peters, K. S. *Acc. Chem. Res.* **1984**, *17*, 277.
(75) Hammond, G. S. *J. Am. Chem. Soc.* **1955**, *77*, 334. See, also: Miller, A. R. *J. Am. Chem. Soc.* **1978**, *100*, 1984.
(76) In which the spin densities at the various positions of $Ar^{\cdot+}$ predict the site of collapse.[51] Lewis, I. C.; Singer, L. S. *J. Chem. Phys.* **1965**, *43*, 2712.
(77) For a discussion, see: Rappoport, Z., Ed.; *Israel J. Chem.* **1987**, *26*, 302, and following papers.

dependence of the reactivity on the electron donor properties of the arene as measured by the ionization potential (vide supra) supports a strong element of, if not complete, electron transfer in the transition state for DT osmylation. Indeed such an interaction derives from the EDA complex that is also the precursor in DT osmylation,[78] as depicted in eq 20 of the electron-transfer formulation below.[80] Although the general outline of the thermal

Scheme IV

$$Ar + OsO_4 \rightleftharpoons [Ar, OsO_4] \quad (19)$$

$$[Ar, OsO_4] \overset{k}{\rightleftharpoons} [Ar^+, OsO_4^-]_s \quad (20)$$

$$[Ar^+, OsO_4^-]_s \xrightarrow{fast} ArOsO_4 \quad (21)$$

mechanism in Scheme IV resembles the charge-transfer mechanism in Scheme II, they differ primarily in the solvation of the ion pair—the adiabatic ion pair in eq 20 being fully solvated (s) in contrast to the nonadiabatic analogue in eq 15.[82] As such, the interionic separation in the adiabatic ion pair is expected to be substantially greater than that formed in eq 15.[83] For example, the exposure of a hexane solution of OsO_4 to the very electron-rich 1,4-dimethoxynaphthalene[84] immediately affords the red-blue EDA complex with the well-defined CT absorption band at λ_{max} 560 nm shown in Figure 10. The solution upon standing gradually turns a bright blue color indicative of the formation of $Ar^{\bullet+}$ according to eq 20.[85] However this arene cation radical is too stable to undergo ion-pair annihilation with OsO_4^-, and no osmylated adduct is observed in competition with back electron transfer.

III. **Comments on the Mechanism of the Promoted Thermal Osmylation of Arenes.** The extensive list of OsO_4 adducts to the arenes included in Table IV underscores the general synthetic utility of PT osmylation. The reactivity trend for various arenes generally follows the order established for DT osmylation, with the benzene derivatives generally being unreactive. PT osmylation differs from DT osmylation in three revealing ways. First, the charge-transfer absorption bands (Table I) are absent, the osmium tetroxide being fully coordinated to pyridine in the form OsO_4(py) as described in eq 8. Second, the rates of osmylation are greatly enhanced, as indicated by the higher conversions attained at shorter reaction times (compare the entries in Tables III and IV). Third, only one isomeric 2:1 adduct **N** and **A** is stereospecifically produced from naphthalene and anthracene, respectively. Since the anti/syn isomers of **N** and **A** are generated from the initially formed 1:1 adduct $ArOsO_4$, the stereospecificity must arise during the rapid addition of the second osmium tetroxide (see Scheme I). The effect of pyridine on this stereochemistry is most likely to derive from the active agent OsO_4(py) that is sterically more encumbered than the free OsO_4 active in the DT process. [A theoretical analysis of the effect of pyridine on alkene osmylation has been recently presented.[86]] The opposed balance between steric hindrance and increased reactivity however appears to be tilted toward the latter. Thus the 2:1 adduct **B** to benzene affords the 3:1 adduct **B′** by PT osmylation but is unreactive to DT osmylation (see Experimental Section). Otherwise the regiospecificities in PT and DT osmylations are indistinguishable as a detailed comparison of the 2:1 adducts in Tables IV and III shows. Most notably the same unusual 2:1 adduct **A** is formed from anthracene by attack of either the five-coordinate OsO_4(py) or the tetrahedral OsO_4. From such similarities we infer that the arenes suffer similar perturbations in the transition state during attack by OsO_4(py) and OsO_4. If so the mechanism presented in Scheme IV is also basically applicable to PT osmylation. Indeed preliminary studies indicate that the dimeric di-9-methylanthracene An_2 undergoes a slow PT osmylation over a period of several days at 60 °C to afford a 30% yield of the adduct from the monomeric methylanthracene listed in Table IV and not the dianthracene adduct, i.e.

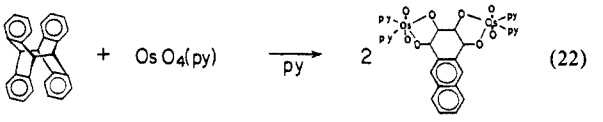

(22)

Such a cycloreversion accompanying PT osmylation accords with the electron-transfer process of An_2 with OsO_4(py) since the cation radical An_2^+ is very short-lived as described in Scheme III.

Summary and Conclusions

The wide-ranging reactivity of various aromatic hydrocarbons to OsO_4 has offered the unique opportunity to probe the activation process for oxidative osmylation, especially with regard to the role of the EDA complex (Table I). In particular, we have shown that the deliberate photoexcitation ($h\nu_{CT}$) of the EDA complex in hexane or dichloromethane effectively activates various arenes including benzenes, naphthalenes, and anthracenes to CT osmylation (Tables V and VI). This photoactivated process is readily associated with the charge-transfer ion pair, i.e.

$$[Ar, OsO_4] \overset{h\nu_{CT}}{\rightleftharpoons} [Ar^{\bullet+}, OsO_4^{\bullet-}] \xrightarrow{fast} ArOsO_4, \text{ etc.}$$

as established by the growth and decay of arene cation radicals (Figure 8) with the aid of time-resolved picosecond spectroscopy (Figures 6 and 7).

When kept in the dark, the same solutions of the EDA complexes slowly afford arene–OsO_4 adducts (Table III) that are identical with those derived by CT osmylation. Indeed the close kinship between the thermal and charge-transfer activation of osmylation is underscored by the unique adduct **A** (Figure 4) in which OsO_4 addition occurs exclusively to the terminal ring and not to the usual meso (9,10-) positions of anthracene.[68-70] The activation process to form the kindred adiabatic ion pair $[Ar^+, OsO_4^-]_s$ in the thermal osmylation provides the unifying theme in arene oxidation. Furthermore the promoted thermal osmylation of arenes via the five-coordinate pyridine analogue OsO_4py (Table IV) is related to the widely used procedure for alkene bishydroxylation.[5] We judge from the same regiochemistry observed, especially with anthracene donors, that the activated complex for PT osmylation is strongly related to that for DT osmylation.

Experimental Section

Materials. Osmium tetroxide (99.5%, Platina Labs) was used as received. Benzene (Mallinkrodt, reagent) was stirred with concentrated H_2SO_4, washed with dilute aqueous NaOH, and distilled from sodiobenzophenone under an argon atmosphere. Naphthalene (Allied, reagent) was recrystallized from ethanol. Phenanthrene (Eastman, reagent) was chromatographed over alumina with benzene, and the middle fraction was recrystallized from benzene/hexane. Anthracene (gold label), 9,10-dimethylanthracene, and 9-bromoanthracene from Aldrich were used as received. The following anthracene derivatives (Aldrich) were recrystallized from the solvents: 9-methyl (methanol), 9,10-dibromo (toluene/hexane), 9-cyano (ethanol), 9-nitro (ethanol/water). 1,4-Dimethylnaphthalene and 1-methoxynaphthalene from Aldrich were used as received, but 2,6-dimethoxynaphthalene was recrystallized from dichloromethane/hexane. 1,4-Dimethoxynaphthalene was prepared from 4-methoxy-1-naphthol by methylation of the potassium salt with methyl iodide, mp 86–7 °C.[87] *cis*-1,2-Dihydrocatechol (*cis*-1,2-dihydroxycyclohexadiene) from Organics Division, Imperial Chemical Industries PLC (UK) was kindly donated by Professor D. Seebach (Zürich) and

(78) It is not possible to show rigorously whether the EDA complex is an obligatory intermediate in DT osmylation. However the point is moot, since its formation is reversible and virtually instantaneous.[12] For a discussion, see ref 79.

(79) Fukuzumi, S.; Kochi, J. K. *J. Am. Chem. Soc.* **1980**, *102*, 2141 (see footnotes 19 and 20).

(80) The mechanism in Scheme IV actually represents one extreme (electron transfer) of a general formulation for electrophilic addition in which eq 20 and 21 are combined in a single step with the ion pair representing a close approximation to the transition state.[81] The other extreme is a concerted electrophilic process with little or no charge development in the transition state.

(81) Kochi, J. K. *Angew. Chem.*, in press.

(82) Fukuzumi, S.; Kochi, J. K. *J. Phys. Chem.* **1980**, *84*, 2254. See also ref 8.

(83) Fukuzumi, S.; Wong, C. L.; Kochi, J. K. *J. Am. Chem. Soc.* **1980**, *102*, 2928.

(84) Mattes, S. L.; Farid, S. *Org. Photochem.* **1983**, *6*, 233.

(85) For analogous colors from stable arene cation radicals, see: Sankararaman, S. et al. in ref 51. See, also: Lau, W.; Kochi, J. K. *J. Am. Chem. Soc.* **1984**, *106*, 7100.

(86) Jørgensen, K. A.; Hoffmann, R. *J. Am. Chem. Soc.* **1986**, *108*, 1867.

used as received. Pyridine (Matheson, Coleman, and Bell, reagent) was stirred over KOH pellets and fractionally distilled, and pyridine-d_5 (Aldrich, gold label) was used as received. *n*-Hexane (Mallinkrodt, reagent) was treated with concentrated H_2SO_4, washed with aqueous $NaHCO_3$, and distilled from sodium. Dichloromethane (Mallinckrodt, reagent) was stirred with concentrated H_2SO_4, washed with aqueous $NaHCO_3$, dried over $CaCl_2$, and distilled from calcium hydride. Carbon tetrachloride (Matheson, Coleman, and Bell, reagent grade glass-distilled) was used as such. All the distillations were carried out under an argon atmosphere.

Instrumentation. UV–vis spectra were recorded on a Hewlett-Packard 8450A diode-array spectrophotometer with 2-nm resolution. Infrared spectra were measured on a Nicolet 10DX FTIR spectrometer. NMR spectra were recorded on either a 90 MHz JEOL FX90Q or a 300 MHz General Electric QE-300 spectrometer. ^1H NMR chemical shifts are reported in ppm downfield from internal TMS standard; ^{13}C NMR chemical shifts are reported in ppm with the central resonance of the solvent peak as reference. Gas chromatographic analyses were performed on a Hewlett-Packard 5790A chromatograph with a 12.5 m SE30 capillary column. GC-MS measurements utilized a Hewlett-Packard 5890 chromatograph interfaced to a HP5970 mass spectrometer (EI, 70 eV). Steady-state photochemical irradiations were performed with the focussed beam from either a 500 W Osram (HBO-2L2) high-pressure Hg lamp or a 1000 W Hanovia (977B0010) Hg-Xe lamp. The light was passed through an IR water filter and an appropriate glass sharp cutoff filter (Corning CS-3 series). The temperature was maintained during the irradiation with the aid of a water bath that consisted of an unsilvered dewar flask.

Preparation of $[OsO_4(C_5H_5N)_2]C_6H_6$ (B_1). A solution of *cis*-1,2-dihydrocatechol (50 mg, 0.45 mmol) in water (1.2 mL) was added to a suspension of $[OsO_2(C_5H_5N)_2(\mu\text{-}O)]_2$[39a] (177 mg, 0.223 mmol) in water (1.0 mL). The pale brown suspension slowly dissolved to give a clear, deep brown solution that produced a pale brown precipitate over a 16-h period. The resulting mixture was evaporated to dryness, washed with diethyl ether, and dried in vacuo. The brown-grey solid was extracted into dichloromethane (3 mL) and filtered, and diethyl ether was added until a light cloudiness was observed. Subsequent cooling of the mixture to −20 °C produced a mass of brown microcrystals that were collected and dried in vacuo: yield of B_1, 0.15 g (69%); IR (KBr, cm^{-1}) 3106 (m), 3076 (m), 3038 (m), 3012 (w), 2861 (m), 2848 (w), 2801 (m), 1606 (s), 1483 (m), 1450 (s), 1209 (m), 1157 (m), 1070 (s), 1026 (s), 999 (s), 952 (m), 936 (s), 873 (m), 832 (vs), 764 (s), 749 (s), 698 (s), 690 (s), 652 (s), 605 (s), 556 (s), 477 (m); ^1H NMR ($CDCl_3$) δ 8.93 (d, 4 H, H-2,6(py), J = 5 Hz), 7.88 (t, 2 H, H-4(py), J = 7 Hz), 7.49 (t, 4 H, H-3,5(py), J = 7 Hz), 6.10 (s, 4 H, H-3,4,5,6), 4.86 (s, 2 H, H-1,2); $^{13}C\{^1H\}$ NMR ($CDCl_3$) δ 149.4, 140.5, 125.2 (py), 129.4 (C-4,5), 124.6 (C-3,6), 85.3 (C-1,2). Elemental Anal. Calcd for $C_{16}H_{16}N_2O_4Os$: C, 39.18; H, 3.29; N, 5.71. Found:[36] C, 38.99; H, 3.33; N, 5.64.

Preparation of $[OsO_4(C_5H_5N)_2]_2C_6H_6$ (B). $[OsO_4(C_5H_5N)_2]C_6H_6$ (0.10 g, 0.20 mmol) was dissolved in dichloromethane (10 mL), and pyridine (28 μL, 0.027 g, 0.35 mmol) was added to give a clear brown solution. Over a 2-min period, a solution of osmium tetroxide (0.044 g, 0.17 mmol) in dichloromethane (5 mL) was added, and the mixture was stirred at room temperature for 20 min. The volume of solvent was reduced to 5 mL under reduced pressure, and excess diethyl ether was added to produce a pale brown precipitate that was collected, washed with diethyl ether (2 × 15 mL), and dried in vacuo. Recrystallization from dichloromethane/diethyl ether afforded brown crystals of B: yield 0.153 g (91%); IR (KBr, cm^{-1}) 3108 (m), 3064 (m), 3045 (m), 3005 (m), 2918 (m), 2893 (m), 2844 (m), 2825 (m), 1607 (s), 1481 (m), 1451 (s), 1210 (m), 1071 (m), 1027 (s), 1014 (s), 935 (w), 898 (m), 869 (m), 832 (vs), 766 (s), 693 (s), 620 (s), 557 (m), 534 (w); ^1H NMR ($CDCl_3$) δ 8.85 (d, 8 H, H-2,6(py), J = 4 Hz), 7.82 (t, 4 H, H-4(py), J = 7 Hz), 7.41 (t, 8 H, H-3,5(py), J = 7 Hz), 6.15 (s, 2 H, H-5,6), 5.30 (s, 1 H, $^1/_2CH_2Cl_2$), 5.26 (s, 2 H) and 5.03 (s, 2 H) (H-1,2,3,4); $^{13}C\{^1H\}$ NMR ($CDCl_3$) δ 149.3, 140.4, 125.1 (py), 129.7 (C-5,6), 88.8, 85.9 (C-1,2,3,4).

Preparation of $[OsO_4(C_5H_5N)_2]_3C_6H_6$ (B′). $[OsO_4(C_5H_5N)_2]C_6H_6$ (0.20 g, 0.41 mmol) was dissolved in dichloromethane (10 mL) to produce a red-brown solution. A solution of osmium tetroxide (0.27 g, 1.1 mmol) in dichloromethane (10 mL) was added, and the mixture was stirred at room temperature for 1 h, whereupon some brown precipitate formed. Pyridine (168 μL, 0.165 g, 2.09 mmol) was added to afford a clear red-brown solution. The solvent was removed under reduced pressure. Dissolution of the sticky solid in dichloromethane (10 mL) and addition of diethyl ether caused a brown powder to precipitate. It was collected and crystallized from nitromethane/diethyl ether to yield 0.43 g (80%) of B′: IR (KBr, cm^{-1}) 3111 (m), 3072 (m), 3046 (m), 3003 (w), 2922 (sh), 2853 (m), 1609 (s), 1483 (m), 1450 (s), 1354 (m), 1245 (w), 1212 (m), 1155 (w), 1070 (s), 1045 (s), 1015 (s), 974 (s), 909 (m), 870 (s), 829 (vs), 764 (s), 695 (s), 641 (s), 611 (s), 589 (s), 457 (w); ^1H NMR (CD_3NO_2) δ 8.82 (d, 12 H, H-2,6(py), J = 5), 7.96 (t, 6 H, H-4(py), J = 7), 7.54 (t, 12 H, H-3,5(py), J = 7), 5.44 (s, 2 H), 5.01 (m, 2 H), 4.79 (br s, 2 H); $^{13}C\{^1H\}$ NMR (CD_3NO_2) δ 150.7, 141.8, 126.6 (py), 93.9, 93.4, 91.1. Elemental Anal. Calcd for $C_{36}H_{36}N_6O_{12}Os_3$: C, 32.87; H, 2.76. Found:[36] C, 31.74; H, 3.13. In an alternative procedure, $[OsO_4(C_5H_5N)_2]_2C_6H_6$ (B) (0.058 g, 0.064 mmol), pyridine (10 μL, 0.128 mmol), and osmium tetroxide (0.017 g, 0.069 mmol) were dissolved in dichloromethane (5 mL), and the brown solution was stirred at room temperature for 2 h. The solvent was removed under reduced pressure to yield a brown powder (0.079 g) that was sparingly soluble in chloroform but dissolved readily in nitromethane. The ^1H NMR spectrum (CD_3NO_2) showed resonances that agreed with those found for B′ above. For the analogous osmylation in the absence of pyridine, $[OsO_4(C_5H_5N)_2]_2C_6H_6$ (B) (0.059 g, 0.065 mmol) and osmium tetroxide (0.018 g, 0.070 mmol) were dissolved in dichloromethane (10 mL) and stirred at room temperature for 2 h. The solvent was removed under reduced pressure so that the unreacted OsO_4 was lost. The brown solid was redissolved in dichloromethane (5 mL), and pyridine (11 μL, 0.14 mmol) was added. The mixture upon workup yielded a brown powder (0.056 g) that was readily soluble in $CDCl_3$. The ^1H NMR spectrum was used to identify the product as unreacted starting material.

Preparation of $[OsO_4(C_5H_5N)_2]_2C_{14}H_{10}$ (A). Anthracene (0.20 g, 1.12 mmol) was dissolved in benzene (10 mL) and osmium tetroxide (0.571 g, 2.25 mmol) and pyridine (0.36 mL, 4.47 mmol) added. The orange solution was left in the dark for 2 days, after which a brown solid formed. It was collected, washed with hexane (3 × 10 mL) and dried in vacuo to yield 0.868 g (72%) of A as the benzene solvate: IR (KBr, cm^{-1}) 3109 (m), 3074 (m), 3043 (m), 3004 (m), 2953 (m), 2918 (m), 2891 (m), 2871 (m), 2852 (m), 1606 (m), 1481 (m), 1450 (s), 1353 (w), 1300 (w), 1213 (m), 1063 (m), 1044 (m), 1009 (m), 1003 (m), 994 (m), 950 (m), 875 (m), 834 (vs), 797 (w), 766 (s), 759 (s), 694 (s), 622 (m), 606 (m), 572 (m), 481 (m); ^1H NMR ($CDCl_3$) δ 8.95 (d, 8 H, H-2,6(py), J = 5 Hz), 8.04 (s, 2 H, H-9,10), 7.79 (t, 4 H, H-4(py), J = 6 Hz), 7.80 (m, 2 H), and 7.33 (m, 2 H) (H-5,6,7,8), 7.45 (t, 8 H, H-3,5(py), J = 6 Hz), 7.36 (s, 6 H, C_6H_6), 5.90 (d, 2 H, J = 4 Hz), and 5.25 (d, 2 H, J = 4 Hz) (H-1,2,3,4); $^{13}C\{^1H\}$ NMR ($CDCl_3$) δ 149.7, 140.2, 125.1 (py), 135.1, 133.6 (quaternary), 128.3, 127.8, 127.5 (C-5,6,7,8,9,10), 92.2, 89.6 (C-1,2,3,4). Elemental Anal. Calcd for $C_{34}H_{30}N_4O_8Os_2 \cdot C_6H_6$: C, 44.44; H, 3.36; N, 5.18. Found:[36] C, 43.54; H, 3.50; N, 5.26.

Promoted Thermal Osmylation. The OsO_4 adducts for the arenes in Table IV were prepared as follows. **Phenanthrene**: Osmium tetroxide (0.518 g, 2.04 mmol) and phenanthrene (0.363 g, 2.04 mmol) were dissolved in pyridine (5.0 mL), and the red-orange solution was left at room temperature in the dark for 13 days. The brown precipitate was collected and washed with hexane (2 × 10 mL). Recrystallization from dichloromethane/pentane afforded brown microcrystals: yield 1.036 g, 75% as the CH_2Cl_2 solvate; IR (KBr, cm^{-1}) 3109 (w), 3059 (m), 3047 (m), 3031 (m), 2977 (w), 2844 (m), 1606 (m), 1481 (m), 1450 (s), 1328 (w), 1216 (w), 1209 (w), 1066 (m), 1044 (m), 994 (m), 956 (m), 938 (m), 894 (w), 875 (m), 834 (vs), 772 (m), 756 (s), 744 (s), 734 (s), 700 (s), 663 (m), 616 (m), 559 (m); ^1H NMR ($CDCl_3$) δ 8.86 (d, 4 H, H-2,6(py), J = 5 Hz), 7.72 (m, 2 H, H-4(py)), 7.43 (m, 4 H, H-3,5(py)), 7.84 (m, 2 H), 7.66 (m, 2 H), and 7.33 (m, 4 H) (H1-8), 5.42 (s, 2 H, H-9,10), 5.25 (s, 2 H, CH_2Cl_2); $^{13}C\{^1H\}$ NMR ($CDCl_3$) δ 149.5, 140.4, 125.2 (py), 135.5, 133.1 (quaternary, 129.2, 128.3, 127.6, 123.4 (C 1-8), 87.9 (C-9,10). Elemental Anal. Calcd for $C_{24}H_{20}N_2O_4Os \cdot CH_2Cl_2$: C, 44.45; H, 3.28; N, 4.15. Found:[36] C, 44.46; H, 3.24; N, 4.27. **9-Methylanthracene.** 9-Methylanthracene (0.119 g, 0.619 mmol) and osmium tetroxide (0.314 g, 1.24 mmol) were dissolved in benzene (5.0 mL) to give a purple solution. Pyridine-d_5 (0.208 g, 2.47 mmol) was added, and the clear red-orange solution was left at room temperature for 6 days in the dark. The brown precipitate was removed, washed with hexane (3 × 10 mL), and dried in vacuo: yield 0.565 g, 82% as the benzene solvate. The product was further purified by recrystallization from dichloromethane/hexane to produce the CH_2Cl_2 solvate as brown microcrystals: IR (KBr, cm^{-1}) 3069 (w), 2907 (m), 2860 (m), 2481 (w), 2365 (w), 2307 (m), 2285 (m), 2265 (m), 1568 (m), 1536 (w), 1384 (w), 1324 (s), 1295 (w), 1054 (w), 1032 (m), 1018 (m), 992 (m), 978 (s), 919 (w), 902 (w), 891 (m), 872 (s), 850 (s), 821 (vs), 800 (m), 781 (w), 762 (m), 745 (m), 731 (w), 679 (w), 660 (w), 631 (m), 615 (m), 596 (m), 569 (m), 536 (s); ^1H NMR ($CDCl_3$) δ 8.07 (m, 1 H), 7.80 (m, 1 H), 7.38 (m, 2 H) (H-5,6,7,8), 7.99 (s, 1 H, H-10), 6.27 (m, 1 H), 5.90 (m, 1 H), 5.17 (m, 2 H) (H-1,2,3,4), 2.89 (s, 3 H, Me); $^{13}C\{^1H\}$ NMR ($CDCl_3$) δ (partial data) 91.2, 89.1, 86.4, 87.1 (C-1,2,3,4), 14.5 (CH_3). Elemental Anal. Calcd for $C_{35}H_{12}D_{20}N_4O_8Os_2 \cdot CH_2Cl_2$: C, 38.53; H, 3.25;[88] N, 4.99. Found:[36] C, 38.87; H, 3.33; N, 5.12. **9,10-Dimethylanthracene.** 9,10-Dimethylanthracene (0.0857 g, 0.415 mmol) and osmium tetroxide (0.211 g, 0.830 mmol) were dissolved in benzene (5.0 mL) to produce a green solution. Pyridine-d_5 (0.140 g, 1.66 mmol) was added, and the

solution was left in the dark for 2 days. The brown precipitate was collected and washed with pentane (3 × 15 mL). Recrystallization from dichloromethane:methanol (1:1) and hexane afforded brown microcrystals: yield 0.323 g, 68% as the CH_2Cl_2 solvate; IR (KBr, cm^{-1}) 3074 (w), 2914 (m), 2859 (m), 2309 (w), 2285 (m), 2266 (w), 1569 (s), 1325 (s), 1297 (w), 1047 (m), 1025 (m), 975 (s), 903 (m), 894 (m), 875 (m), 850 (s), 834 (s), 822 (vs), 766 (m), 747 (m), 656 (m), 634 (m), 616 (m), 600 (m), 588 (m), 563 (m), 534 (s), 425 (w); ^1H NMR ($CDCl_3$) δ 8.09 (m, 2 H), 7.42 (m, 2 H) (H-5,6,7,8), 6.21 (m, 2 H), 5.20 (m, 2 H) (H-1,2,3,4), 2.88 (s, 6 H, $2CH_3$); $^{13}C\{^1H\}$ NMR ($CD_3OD/CDCl_3$) δ (partial data) 133.0, 131.3 (quaternary, 125.1, 124.5 (C-5,6,7,8), 89.1, 83.9 (C-1,2,3,4), 14.2 ($2CH_3$). Elemental Anal. Calcd for $C_{36}H_{14}D_{20}N_4O_8Os_2 \cdot CH_2Cl_2$: C, 39.11; H, 3.39;[88] N, 4.93. Found:[36] C, 38.90; H, 3.79; N, 4.99. **9-Methoxyanthracene.** 9-Methoxyanthracene (0.108 g, 0.519 mmol) and osmium tetroxide (0.264 g, 1.04 mmol) were dissolved in benzene (5.0 mL), and pyridine-d_5 (178 μL, 2.07 mmol) was added. After 4 days, a solid brown mass of microcrystals formed, which were collected, washed with benzene and hexane (2 × 20 mL), and dried in vacuo: yield 0.452 g, 83%; IR (KBr, cm^{-1}) 3065 (w), 2931 (m), 2899 (m), 2842 (m), 2483 (w), 2309 (w), 2288 (m), 2265 (w), 2229 (w), 1567 (s), 1370 (w), 1324 (s), 1302 (sh), 1240 (w), 1086 (m), 1024 (sh), 1012 (m), 979 (s), 909 (w), 888 (m), 872 (m), 851 (s), 833 (sh), 821 (vs), 750 (m), 654 (m), 604 (m, br), 536 (s), 421 (w); ^1H NMR ($CDCl_3$) δ 8.10 (m, 1 H), 7.77 (m, 1 H), and 7.3 (m, 2 H) (H-5,6,7,8), 7.90 (s, 1 H, H-10), 6.58 (d, 1 H, J = 5 Hz), 5.87 (d, 1 H, J = 5 Hz), 5.35 (m, 1 H), and 5.08 (m, 1 H) (H-1,2,3,4), 4.10 (s, 3 H) (CH_3). Elemental Anal. Calcd for $C_{35}H_{12}D_{20}N_4O_9Os_2$: C, 39.91; H, 3.28; N, 5.32. Found:[36] C, 39.47; H, 3.13; N, 5.17. **9,10-Dibromoanthracene.** Osmium tetroxide (0.234 g, 0.920 mmol) and 9,10-dibromoanthracene (0.155 g, 0.460 mmol) were dissolved in benzene (5.0 mL) to give a red-orange solution. Pyridine-d_5 (158 μL, 1.84 mmol) was added, and the mixture was left in the dark for 14 days. The brown precipitate that had formed was collected and washed with benzene (2 × 10 mL) and hexane (2 × 10 mL). Upon drying the solid in vacuo, it afforded 0.417 g (72%) of brown powder as the benzene solvate: IR (KBr, cm^{-1}) 3089 (w), 3066 (w), 3033 (w), 2895 (m), 2864 (m), 2308 (m), 2281 (m), 2263 (m), 1567 (s), 1536 (w), 1478 (m), 1325 (s), 1284 (w), 1252 (m), 1241 (w), 1167 (w), 1069 (w), 1035 (s), 1017 (s), 979 (s), 939 (m), 924 (m), 901 (m), 890 (m), 876 (s), 851 (s), 835 (s), 820 (vs), 778 (w), 758 (s), 737 (w), 726 (s), 681 (s), 621 (s), 613 (s), 593 (s), 561 (m), 536 (s); ^1H NMR ($CDCl_3$) δ 8.44 (m, 2 H) and 7.55 (m, 2 H) (H-5,6,7,8), 7.36 (s, 6 H, C_6H_6), 6.37 (m, 2 H), and 5.23 (m, 2 H) (H-1,2,3,4). Elemental Anal. Calcd for $C_{40}H_8D_{20}Br_2N_4O_8Os_2 \cdot C_6H_6$: C, 38.16; H, 2.88; N, 4.45. Found:[36] C, 39.28; H, 2.85; N, 4.40. **Naphthalene.** (a) Naphthalene (0.100 g, 0.78 mmol) and osmium tetroxide (0.397 g, 1.6 mmol) were dissolved in benzene (7.5 mL) to yield an orange solution. Pyridine (251 μL, 3.1 mmol) was added, and the yellow solution was left in the dark for 8 days. After this time very little reaction had occurred, as judged by the miniscule precipitate, and a further 1.0-mL aliquot of pyridine was added. After a total of 30 days, the brown precipitate was collected, washed with benzene (2 × 10 mL) and hexane (2 × 10 mL), and dried in vacuo: yield 0.231 g, 29% as the benzene solvate. A sample was recrystallized from dichloromethane/methanol (1:1) and hexane for characterization: IR (KBr, cm^{-1}) 3107 (w), 3072 (m), 3044 (m), 3002 (w), 2847 (br, m), 1607 (s), 1483 (m), 1450 (s), 1209 (m), 1068 (m), 1047 (m), 1012 (m), 991 (m), 950 (w), 935 (m), 896 (w), 873 (m), 833 (vs), 764 (s), 694 (s), 649 (w), 629 (w), 597 (w), 574 (w). Elemental Anal. Calcd for $C_{30}H_{28}N_4O_8Os_2 \cdot {}^1/_2CH_2Cl_2$: C, 36.80; H, 2.94; N, 5.63. Found:[36] C, 36.76; H, 2.90; N, 5.70. (b) By using a procedure similar to (a), a mixture of osmium tetroxide (0.167 g, 0.658 mmol), naphthalene (0.042 g, 0.328 mmol) and pyridine-d_5 (113 μL, 1.32 mmol) was allowed to react in benzene (5.0 mL) for 70 days: yield of brown microcrystals 0.180 g, 52% as the benzene solvate; IR (KBr, cm^{-1}) 3089 (w), 3071 (m), 3031 (m), 2904 (m), 2888 (w), 2826 (m), 2285 (m), 2266 (sh), 1567 (m), 1325 (s), 1062 (w), 1017 (m), 991 (m), 977 (m), 935 (m), 876 (m), 852 (m), 837 (s), 823 (vs), 773 (s), 761 (m), 706 (w), 681 (m), 649 (s), 629 (m), 614 (m), 596 (m), 572 (s), 538 (s), 423 (w); ^1H NMR ($CDCl_3$) δ 7.80 (m, 2 H) and 7.54 (m, 2 H) (H-5,6,7,8), 7.37 (s, 6 H, C_6H_6), 5.75 (d, 2 H, J = 4) and 5.22 (d, 2 H, J = 4) (H-1,2,3,4); $^{13}C\{^1H\}$ NMR ($CDCl_3/CD_3OD$) δ 135.9, 129.2, 128.1, 89.6, 87.3. **1,4-Dimethylnaphthalene.** Osmium tetroxide (0.267 g, 1.05 mmol), 1,4-dimethylnaphthalene (0.082 g, 0.526 mmol), and pyridine-d_5 (180 μL, 2.10 mmol) were dissolved in benzene (5.0 mL), and the mixture was allowed to react in the dark for 14 days. The brown precipitate was collected, washed with benzene (2 × 15 mL) and hexane (3 × 10 mL), and air dried. Recrystallization from dichloromethane/methanol (1:1) and hexane gave 0.113 g (20%) of brown microcrystals as the dichloromethane solvate: IR (KBr, cm^{-1}) 2969 (m), 2922 (m), 2856 (m), 2289 (m), 2262 (w), 1569 (m), 1325 (s), 1159 (w), 1084 (w), 1059 (w), 1013 (m), 978 (m), 959 (w), 909 (w), 888 (w), 872 (m), 850 (m), 834 (m), 819 (vs), 744 (s), 694 (m), 669 (w), 628 (s), 616 (m), 588 (w), 563 (m), 534 (m); ^1H NMR ($CDCl_3$) δ 7.56 (m, 2 H) and 7.26 (m, 2 H) (H-5,6,7,8), 5.45 (s, 2 H, H-2,3), 5.30 (s, 2 H, CH_2Cl_2), 1.98 (s, 6 H, 2Me). Elemental Anal. Calcd for $C_{32}H_{32}N_4O_8Os_2 \cdot {}^1/_2CH_2Cl_2$: C, 38.14; H, 3.25; N, 5.47. Found:[36] C, 38.04; H, 3.31; N, 5.50. **1-Methoxynaphthalene.** Osmium tetroxide (0.442 g, 1.74 mmol), 1-methoxynaphthalene (0.137 g, 0.866 mmol), and pyridine-d_5 (298 μL, 3.48 mmol) were dissolved in benzene (5.0 mL) to yield an orange solution. This mixture was left at room temperature in the dark for 37 days. The brown microcrystalline deposit was collected, washed with benzene (2 × 15 mL), and dried in vacuo: yield 0.636 g, 73%; IR (KBr, cm^{-1}) 3066 (w), 3031 (w), 2965 (m), 2934 (m), 2895 (m), 2482 (w), 2290 (m), 2267 (w), 2229 (w), 1568 (m), 1560 (m), 1326 (s), 1099 (w), 1038 (m), 1016 (m), 1005 (w), 975 (s), 914 (m), 877 (m), 853 (s), 821 (vs), 767 (m), 667 (m), 611 (m), 589 (m), 538 (s); ^1H NMR ($CDCl_3$) δ 7.81 (m, 2 H) and 7.60 (m, 2 H) (H-5,6,7,8), 7.26 (s, 6 H, C_6H_6), 5.73 (d, 1 H, J = 5), 5.42 (d, 1 H, J = 5), and 5.24 (m, 1 H) (H-2,3,4), 3.61 (s, 3 H, OMe). Elemental Anal. Calcd for $C_{31}H_{10}D_{20}N_4O_9Os_2$: C, 37.12; H, 3.24; N, 5.59. Found:[36] C, 36.06; H, 2.89; N, 5.61. **2,6-Dimethoxynaphthalene.** A mixture of osmium tetroxide (0.280 g, 1.10 mmol) and 2,6-dimethoxynaphthalene (0.104 g, 0.550 mmol) was dissolved in benzene (5.0 mL), and pyridine-d_5 (188 μL, 2.20 mmol) was added. The resulting yellow solution was left at room temperature in the dark for 37 days. The deposited brown material was collected, washed with benzene (2 × 10 mL) and hexane (2 × 10 mL), and dried in vacuo: yield 0.388 g, 61% as the benzene solvate; IR (KBr, cm^{-1}) 3086 (w), 3068 (w), 3056 (w), 3031 (w), 3003 (w), 2982 (w), 2954 (m), 2940 (m), 2904 (m), 2886 (m), 2858 (w), 2829 (w), 2482 (w), 2309 (sh), 2286 (m), 2264 (m), 2229 (w), 1609 (m), 1569 (m), 1536 (w), 1495 (m), 1478 (w), 1465 (w), 1384 (w), 1325 (s), 1288 (w), 1254 (m), 1230 (m), 1192 (w), 1160 (w), 1128 (w), 1077 (s), 1043 (m), 1037 (m), 1004 (m), 989 (m), 978 (s), 955 (w), 909 (w), 890 (w), 873 (m), 865 (m), 855 (s), 819 (vs), 805 (m), 754 (m), 693 (m), 640 (w), 609 (s), 560 (m), 539 (s), 426 (w), 418 (w); ^1H NMR ($CDCl_3$) δ 7.49 (d, 1 H, J = 9 Hz, H-8), 7.12 (d, 1 H, J = 3 Hz, H-5), 6.84 (dd, 1 H, J = 3, 9 Hz, H-7), 5.66 (d, 1 H, J = 4 Hz, H-4), 5.44 (s, 1 H, H-1), 5.31 (d, 1 H, J = 4 Hz, H-3), 3.78 (s, 3 H, OMe), 3.65 (s, 3 H, OMe). Elemental Anal. Calcd for $C_{32}H_{12}D_{20}N_4O_{10}Os_2 \cdot {}^3/_2C_6H_6$: C, 42.81; H, 3.79; N, 4.87. Found:[36] C, 42.67; H, 3.54; N, 4.94. **9-Bromoanthracene.** 9-Bromoanthracene (0.0735 g, 0.286 mmol) and osmium tetroxide (0.145 g, 0.572 mmol) were dissolved in benzene (5.0 mL), and pyridine-d_5 (101 μL, 1.176 mmol) was added. After 10 days in the dark, a brown crystalline mass had formed, which was collected, washed with benzene (2 × 10 mL) and hexane (2 × 10 mL), and dried in vacuo: yield 0.244 g, 78%; IR (KBr, cm^{-1}) 3065 (w), 3051 (w), 3027 (w), 2898 (m), 2874 (m), 2850 (m), 2483 (w), 2371 (w), 2308 (w), 2289 (m), 2264 (w), 2229 (w), 1568 (s), 1536 (w), 1490 (w), 1325 (s), 1309 (br, w), 1250 (w), 1067 (w), 1029 (m), 1007 (m), 999 (m), 979 (s), 953 (m), 890 (m), 876 (s), 852 (s), 833 (s), 822 (vs), 798 (w), 756 (w), 743 (w), 716 (w), 694 (w), 661 (m), 649 (m), 614 (s), 573 (s), 538 (s), 497 (w); ^1H NMR ($CDCl_3$) δ 8.29 (m, 1 H), 7.79 (m, 1 H) and 7.42 (m, 2 H) (H-5,6,7,8), 8.08 (s, 1 H, H-9), 6.54 (d, 1 H, J = 5 Hz), 5.88 (dd, 1 H, J = 1, 5 Hz), and 5.22 (eight lines, 2 H) (H-1,2,3,4). Elemental Anal. Calcd for $C_{34}H_9D_{20}BrN_4O_8Os_2$: C, 37.05; H, 2.86; N, 5.08. Found:[36] C, 37.22; H, 2.77; N, 4.94. **9-Cyanoanthracene.** Osmium tetroxide (0.1803 g, 0.709 mmol) and 9-cyanoanthracene (0.0721 g, 0.355 mmol) were dissolved in benzene (5.0 mL), and pyridine-d_5 (122 μL, 1.42 mmol) was added. After 12 days the brown microcrystals were collected, washed with benzene (2 × 10 mL) and hexane (3 × 10 mL), and then dried in vacuo: yield 0.312 g, 78% as the benzene solvate; IR (KBr, cm^{-1}) 3089 (w), 3068 (w), 3034 (m), 2870 (m), 2484 (w), 2310 (w), 2287 (m), 2264 (w), 2217 (m), 1568 (s), 1538 (w), 1499 (w), 1479 (m), 1325 (s), 1295 (w), 1241 (w), 1203 (w), 1100 (w), 1057 (m), 1041 (m), 1026 (m), 1006 (m), 993 (m), 978 (s), 942 (w), 911 (w), 888 (m), 875 (s), 852 (s), 834 (s), 822 (vs), 791 (m), 773 (m), 758 (w), 747 (w), 706 (w), 683 (m), 648 (m), 607 (m), 586 (s), 535 (s), 464 (w); ^1H NMR ($CDCl_3$) δ 8.29 (s, 1 H, H-10), 8.25 (m, 1 H), 7.88 (m, 1 H) and 7.51 (m, 2 H) (H-5,6,7,8), 7.36 (s, 6 H, C_6H_6), 6.26 (d, 1 H, J = 4 Hz), 5.83 (d, 1 H, J = 4 Hz) and 5.29 (m, 2 H), (H-1,2,3,4). Elemental Anal. Calcd for $C_{41}H_{15}D_{20}N_5O_8Os_2$: C, 43.72; H, 3.33; N, 6.22. Found:[36] C, 43.63; H, 3.26; N, 5.96. **9-Nitroanthracene.** 9-Nitroanthracene (0.0656 g, 0.294 mmol) and osmium tetroxide (0.1495 g, 0.588 mmol) were dissolved in benzene (5.0 mL), and pyridine-d_5 (101 μL, 1.18 mmol) was added. After 12 days the deposited brown needles were collected, washed with benzene (2 × 10 mL) and hexane (2 × 10 mL), and dried in high vacuum: yield 0.2404 g, 71% as the benzene solvate; IR (KBr, cm^{-1}) 3088 (w), 3060 (w), 3034 (w), 2884 (m), 2847 (m), 2481 (w), 2304 (w), 2286 (w), 2262 (w), 1569 (m), 1527 (s), 1385 (w), 1368 (w), 1341 (w), 1326 (s), 1301 (m), 1265 (w), 1051 (s), 1027 (w), 1009 (m), 978 (m), 923 (w), 888 (m), 881 (m), 854 (s), 836 (s), 822 (vs), 774 (w), 755 (m), 742 (w), 729 (w), 684 (w), 646 (w), 638 (w), 607 (s), 582 (w), 534 (m),

419 (w); ^{1}H NMR ($CDCl_3$) δ 8.23 (s, 1 H, H-10), 7.85 (d, 1 H, J = 7 Hz), 7.73 (d, 1 H, J = 8 Hz), 5.97 (d, 1 H, J = 5 Hz), 5.71 (dd, 1 H, J = 5, 0.6 Hz), 5.52 (t, 1 H, J = 4 Hz), 5.43 (dd, 1 H, J = 5, 4 Hz) (H-1,2,3,4). Elemental Anal. Calcd for $C_{37}H_{12}D_{20}N_5O_{10}Os_2$: C, 40.14; H, 3.12; N, 6.33. Found:[36] C, 39.67; H, 2.88; N, 6.31.

Direct Thermal Osmylation. Typically the reactions in alkane solvents were carried out in the dark by heating them in sealed ampoules or allowing them to stand for prolonged periods as described for the following arenes. **Anthracene.** A mixture of osmium tetroxide (0.215 g, 0.84 mmol), anthracene (0.076 g, 0.43 mmol), and heptane (5.0 mL) was placed in an ampoule that was then sealed in vacuo. The pale purple solution was heated to 100 °C in the dark for 32 h, whereupon a large amount of orange-brown precipitate formed. It was collected and treated with a solution of pyridine-d_5 (145 μL, 1.7 mmol) in CH_2Cl_2 (5 mL). The resulting brown solution was filtered and treated with diethyl ether to yield a pale brown precipitate that was dried in vacuo: yield 0.295 g, 68%. Elemental Anal. Calcd for $C_{34.5}H_{11}D_{20}ClN_4O_8Os_2$: C, 38.88; H, 3.14;[88] N, 5.26. Found:[36] C, 39.06; H, 3.02; N, 5.26. Although this product had an elemental analysis consistent with a 2:1 adduct, ^{1}H NMR analysis indicated the presence of two isomers. The major isomer showed the characteristic resonances that were identical with those of the anti adduct **A** from the osmylation of anthracene in the presence of pyridine, viz: δ 8.03 ppm (2 H), 7.81 (2 H), 7.34 (2 H), 5.88 (2 H), 5.23 (2 H). The minor isomer assigned to the syn adduct showed resonances at δ 8.12 ppm (s, 2 H), 5.63 (br s, 4 H); the aromatic resonances were obscured by the resonances due to solvent and the other stereoisomer. The two isomers **A** and syn-**A** were present in a ratio of 2:1. The corresponding $^{13}C\{^1H\}$ NMR spectrum showed carbon (ester) resonances for isomer **A** at 91.6 and 89.6 ppm and for syn-**A** at 88.9 and 88.3 ppm. When a similar mixture of anthracene and OsO_4 in hexane was left at room temperature in the dark for 51 days, it precipitated a brown solid. Derivatization of the solid with pyridine afforded a 10% yield of the mixture of **A** (60%) and syn-**A** (40%), as determined by ^{1}H NMR analysis. **Naphthalene.** A mixture of naphthalene (0.077 g, 0.60 mmol) and osmium tetroxide (0.304 g, 1.20 mmol) was dissolved in heptane (5.0 mL) and sealed in an ampoule in vacuo. The bright yellow solution was heated to 100 °C in the dark for 5.5 days. After this time, a small amount of brown precipitate formed, which was collected and treated with a solution of pyridine-d_5 (0.1 mL, 1.17 mmol) in dichloromethane (5 mL). The solution was filtered and concentrated to yield ca. 20 mg (3%) of a brown solid. ^{1}H NMR analysis in CD_3CN showed resonances due to the anti stereoisomer **N** (Table IV) at δ 7.42 ppm (2 H), 7.29 (2 H), 5.36 (2 H), 4.72 (2 H) together with another set of resonances at δ 7.45 ppm (2 H), 7.21 (2 H), 5.28 (2 H), 5.10 (2 H) for the syn isomer. From the integrals of the two sets of resonances, we judged that more or less equimolar amounts of **N** and syn-**N** were formed. **Phenanthrene.** A mixture of phenanthrene (0.092 g, 0.52 mmol) and osmium tetroxide (0.131 g, 0.52 mmol) was dissolved in hexane (5.0 mL), and the yellow mixture was stored in the dark for 43 days. After this time a solution of pyridine (1 mL) in benzene (5 mL) was added, and the resulting brown solution was filtered. Addition of diethyl ether caused the precipitation of a brown powder which was recrystallized from dichloromethane/diethyl ether: yield 0.025 g, 7%. The ^{1}H NMR spectrum of the product was identical with that (**P**) formed by the treatment of phenanthrene with osmium tetroxide in the presence of pyridine (vide supra). **1,4-Dimethylnaphthalene.** A mixture of 1,4-dimethylnaphthalene (0.038 g, 0.24 mmol) and osmium tetroxide (0.123 g, 0.48 mmol) was dissolved in hexane (5.0 mL) to yield an orange solution. After storage in the dark for 51 days, the resulting dark solid was removed, washed with diethyl ether (2 × 10 mL), and dried in vacuo. Addition of a solution of pyridine (0.5 mL) in dichloromethane yielded a brown solution, which was filtered and treated with excess diethyl ether to give a brown precipitate. The solid was collected and dried: yield 0.02 g, 8%. The ^{1}H NMR spectrum of the product was shown to be exclusively the anti 2:1 adduct N_{m2} by comparison of the ^{1}H NMR spectrum with that prepared by PT osmylation (see Table IV).

Charge-Transfer Osmylation. All photochemical reactions were carried out by the same general procedure. Solutions of the aromatic substrate and osmium tetroxide were prepared in the desired solvent (hexane, tetrachloromethane, or dichloromethane). Usually the OsO_4 was employed in molar excess in order to maximize the absorbances of the charge-transfer band. The solutions were irradiated by using an appropriate cut-off filter, such that only the charge-transfer bands were excited. For experiments of longer duration, the sample was periodically centrifuged and transferred to a fresh tube to minimize absorption of light by the precipitated product. After a known period of irradiation, the precipitated material was collected, and the mother liquor was analyzed by gas chromatography for the presence of new organic products. The precipitate was treated with either pyridine or pyridine-d_5 and stirred for 2 h. After dilution with dichloromethane (5 mL), the brown solution was filtered and treated with diethyl ether to precipitate the product as a pale brown powder, which was dried and characterized by comparison with the products of thermal osmylation of the same substrate. **Anthracene in Hexane.** A mixture of anthracene (0.22 g, 0.12 mmol) and osmium tetroxide (0.26 g, 1.01 mmol) was dissolved in hexane (3.0 mL) to give a purple solution. The solution was irradiated for a total of 17 h with a 1 kW Hg-Xe lamp at wavelengths greater than 480 nm. The solution was occasionally agitated to remove a black solid material that blocked the path of the light beam. After this time the solution was centrifuged, and the volume of the purple mother liquor was reduced in vacuo to leave a white solid. GC analysis of the solid dissolved in dichloromethane indicated the formation of anthraquinone (0.002 mmol). The anthraquinone was positively identified by co-injection of a sample containing authentic anthraquinone and by GC-MS analysis that showed the parent ion at m/z = 208. The residual black solid (2.4 mg) was found to be insoluble in all common organic solvents, pyridine, and water. It did however dissolve in concentrated nitric acid and sodium hypochlorite. It was analyzed by dissolution in concentrated HCl to give the hexachloroosmate(IV), following the stoichiometry: $OsO_2 + 6HCl \rightarrow H_2OsCl_6 + 2H_2O$. The green hexachloroosmate was determined spectrophotometrically, by using an authentic sample of OsO_2, prepared from reduction of OsO_4 with ethanol, as the reference. Thus, a known weight of authentic OsO_2 (0.0107 g) was dissolved in concentrated HCl. The resulting deep green solution was diluted to 250.0 mL with concentrated HCl, and the absorbances at 339 nm (ϵ 5710 M^{-1} cm^{-1}) and 374 nm (ϵ 5410 M^{-1} cm^{-1}) were measured. A sample of the unknown (0.00127 g) was treated similarly, and the measurements of the absorbances at 339 and 374 nm were 1.172 and 1.152, which correspond to 90% and 93% of the expected values, respectively. **Anthracene in Dichloromethane.** A mixture of anthracene (0.06 g, 0.34 mmol) and osmium tetroxide (0.29 g, 1.15 mmol) was dissolved in dichloromethane (5.0 mL) and irradiated with the output from a 1000 W Hg-Xe lamp at wavelengths greater than 480 nm for 5.5 h. The original purple solution turned a brown color, and the volatiles were removed in vacuo. The resulting pale brown solid was washed with hexane (5 × 10 mL) and then dissolved in pyridine (2 mL). After stirring for 30 min, the brown solution was treated with hexane to produce a brown precipitate. It was collected, washed with hexane (3 × 10 mL), and dried in vacuo: yield 20 mg. ^{1}H NMR analysis of the product ($CDCl_3$) indicated the presence of the anti stereoisomer **A** of the 2:1 adduct with characteristic resonances at δ 8.03 ppm (2 H), 7.81 (2 H), 7.34 (2 H), 5.88 (2 H), 5.23 (2 H), together with the characteristic resonances of syn-**A** at 8.12 ppm (2 H), 5.63 (4 H), (vide supra). The product distribution of 50% **A** and 50% syn-**A** compared well with that found in the DT osmylation of anthracene. **Naphthalene in Hexane.** Irradiation of naphthalene (0.10 g, 0.78 mmol) and osmium tetroxide (0.15 g, 0.59 mmol) in hexane (3.0 mL) at wavelengths greater than 415 nm for 8.5 h, resulted in the precipitation of a brown material. Treatment with pyridine-d_5 (0.5 mL) gave a brown osmate ester (0.023 mmol) which was shown by ^{1}H NMR spectroscopy to be a mixture of **N** (75%) and syn-**N** (25%). The ^{1}H NMR spectrum consisting of the two components concurred with that found from the DT osmylation of naphthalene (vide supra). **Naphthalene in Dichloromethane.** By using a similar procedure, naphthalene (0.078 g, 0.61 mmol) and OsO_4 (0.23 g, 0.90 mmol) were irradiated in dichloromethane at wavelengths greater than 415 nm for 7.5 h. The resulting yellow-brown solution was treated with pyridine to yield a brown osmate ester (0.005 mmol). ^{1}H NMR analysis showed the presence of a pair of 2:1 adducts with a composition consisting of 57% **N** and 43% syn-**N**. **1,4-Dimethylnaphthalene.** A mixture of 1,4-dimethylnaphthalene (0.106 g, 0.68 mmol) and OsO_4 (0.145 g, 0.57 mmol) was dissolved in hexane (3.0 mL) to give an orange solution. Irradiation at > 425 nm for 4.25 h gave a brown precipitate, which on treatment with pyridine yielded 0.05 mmol of the 2:1 adduct 1,4-$C_{12}H_{12}$·2OsO_4·4py. This product was shown to consist exclusively of the anti stereoisomer by ^{1}H NMR spectroscopy in comparison with the product formed by thermal osmylation of 1,4-dimethylnaphthalene. **Phenanthrene.** A solution of phenanthrene (0.148 g, 0.83 mmol) and OsO_4 (0.25 g, 0.98 mmol) in tetrachloromethane (3.0 mL) was irradiated at wavelengths greater than 380 nm for 8.75 h. Treatment of the resulting brown precipitate with pyridine yielded 0.10 mmol of the 1:1 adduct **P** $C_{14}H_{10}$·OsO_4·2py, as confirmed by comparison of its ^{1}H NMR spectrum with that of an authentic sample. **Other Charge-Transfer Osmylations in (3.0 mL) Hexane: 9-bromoanthracene** (0.12 mmol), OsO_4 (0.36 mmol), λ > 480 nm; 4.75 h yielded OsO_2 (0.029 mmol), anthraquinone (0.012 mmol); **9,10-dibromoanthracene** (0.083 mmol), OsO_4 (0.90 mmol), λ > 480 nm; 3.25 h yielded OsO_2 (0.053 mmol), anthra-

(87) Baker, B. R.; Carlson, G. H. *J. Am. Chem. Soc.* **1942**, *64*, 2567.
(88) Corrections for ^{2}H analysis that were experimentally determined as ^{1}H (water) were made here and in all subsequent adducts that contained pyridine-d_5 as ligands.

quinone (0.033 mmol); **9-nitroanthracene** (0.13 mmol), OsO_4 (0.99 mmol), $\lambda > 480$ nm, 18 h gave OsO_2 (0.019 mmol), anthraquinone (0.015 mmol); **9-cyanoanthracene** (0.025 mmol), OsO_4 (0.98 mmol), $\lambda > 480$ nm, 5.5 h yielded OsO_2 (0.004 mmol), no other products detected; **2,6-dimethoxynaphthalene** (0.072 mmol), OsO_4 (0.60 mmol), $\lambda > 425$ nm, 18.5 h gave OsO_2 (0.007 mmol); **1-Methoxynaphthalene** (0.28 mmol), OsO_4 (0.57 mmol), $\lambda > 425$ nm, 12.25 h gave OsO_2 (0.009 mmol); **9,10-dimethylanthracene** (0.32 mmol), OsO_4 (0.64 mmol, $\lambda > 480$ nm, 12.25 h yielded a mixture of 2:1 adducts (0.008 mmol) after pyridine workup consisting of 15% syn adduct (^{1}H NMR δ 6.03 (2 H, m), 5.56 (2 H, m)) and 85% anti adduct (^{1}H NMR δ 6.23 (2 H, m), 5.22 (2 H, m)); **9-methylanthracene** (0.32 mmol), OsO_4 (0.32 mmol), $\lambda > 480$ nm, 12.25 h, gave a mixture of a pair of 2:1 adducts after pyridine workup (0.015 mmol): 50% syn adduct (^{1}H NMR δ 8.07 (1 H, s, **H-10**), 6.17 (1 H, m), 5.73 (1 H, m), 5.59 (1 H, m)) and 50% anti adduct (^{1}H NMR δ 7.99 (1 H, s, H-10), 6.27 (1 H, m), 5.89 (1 H, m), 5.22 (1 H, m)). **Other Charge-Transfer Osmylations in (3.0 mL) Dichloromethane: 2,6-dimethoxynaphthalene** (0.36 mmol), OsO_4 (0.76 mmol), $\lambda > 415$ nm, 10 h, no reaction; **1-methoxynaphthalene** (0.28 mmol), OsO_4 (0.57 mmol), $\lambda > 425$ nm, 12.25 h gave a trace amount of OsO_2 (<0.001 mmol); **9,10-dimethylanthracene** (0.32 mmol), OsO_4 (0.64 mmol), $\lambda > 480$ nm, 12.25 h, yielded a mixture of two isomers of 2:1 adduct (0.010 mmol): 44% syn adduct and 56% anti adduct; ^{1}H NMR spectra were similar to those from the photochemical reaction in hexane; **9,10-dibromoanthracene** (0.12 mmol), OsO_4 (0.36 mmol), $\lambda > 480$ nm, 4.75 h, yielded traces of the 2:1 adduct; **9-nitroanthracene** (0.13 mmol), OsO_4 (0.99 mmol), $\lambda > 480$ nm, 18 h, gave no reaction.

Time-Resolved Spectroscopy for Charge-Transfer Osmylation. The transient intermediates formed during the photoexcitation of the EDA complexes of arenes and OsO_4 were examined in two time regimes. Time-resolved differential absorption spectra in the picosecond time scale were obtained by using a laser-flash system that utilized the 532-nm second harmonic 30-ps (fwhm) pulses from a Quantel YG402 mode-locked Nd:YAG laser as the excitation source (~10 mJ per pulse). The analyzing beam was produced by passing the fundamental wavelength (1064 nm) through a solution of phosphoric acid in D_2O, to generate a pulse of white light.[89] Temporal measurements were made by varying the pathlength of the fundamental with respect to the second harmonic.[90] Spectra were measured for each time by averaging 25 individual pulses. Measurements were made at times less than and greater than the maximum absorbance for the transient, such that t_0 could be determined as the time at which the absorbance due to the transient had reached half-maximum. Time-resolved differential absorption spectra in the ns–μs time regime were measured on a laser flash system based on the Quantel YG580-10 Q-switched Nd:YAG laser with a pulse width of 10 ns (fwhm). The 1064-nm pulse was frequency doubled and separated with a dichroic mirror to obtain 532-nm pulses of 160–170 mJ. The interrogating beam consisted of the output from a 150 W xenon lamp in a Oriel lamp housing with a Aspherab UV grade condenser lens. The emerging probe beam was focussed onto an Oriel 77250 monochromator. A Hamamatsu R928 photomultiplier tube attached to the exit slit of the monochromator served as the detector. A Kinetic Instruments sequence generator and laser controller was used in conjunction with a Tektronix 7104 oscilloscope – C101 video camera for digitizing. The data acquisition was performed with Tektronix DCS01 software in an AT&T 6300 plus computer for processing with ASYST 2.0 software.

Quantum Yield for Charge-Transfer Osmylation. Quantum yields were determined by a standard procedure, as exemplified by the CT osmylation of anthracene. A 1000 W Hg-Xe lamp was equipped with an infrared water filter, and an appropriate narrow band-pass interference filter (e.g., 520 ± 5 nm). The light intensity was measured with a Reinecke salt actinometer[48] in which $K[Cr(NCS)_4(NH_3)_2]$ (ca. 50 mg) was dissolved in distilled water (5 mL), and the solution was filtered in the dark. One 2.0-mL aliquot served as a blank to monitor the dark, thermal reaction. A second 2.0-mL aliquot was photolyzed for typically 10.0 min with constant stirring. A 1.0-mL aliquot of each solution was then diluted to 5.0 mL with an aqueous solution of iron(III) nitrate (0.1 M) containing perchloric acid (0.5 M) and left to develop for 30 min. The difference in absorbance at 450 nm between the photolyzed and blank solutions was used to calculate the number of einstein emitted per second at the monitoring wavelength. To a solution of the appropriate arene (ca. 0.02 mM) in dichloromethane or hexane (3.0 mL) was added excess OsO_4 (ca. 5 mM). A 1.0-mL aliquot was removed and added to an aqueous solution of sodium bisulfite (ca. 1 g in 10 mL). After the unreacted OsO_4 was destroyed, the aqueous layer was extracted with the corresponding solvent. The extracts were combined to a total volume of 50.0 mL. The concentration of the arene was then determined spectrophotometrically. The remaining 2.0 mL of solution was then irradiated for a known period of time (typically 3 h), and a second 1.0-mL aliquot was removed and treated identically to the first aliquot. From the change in concentration of the aromatic hydrocarbon, the quantum yield at the monitoring wavelength was calculated. The alternative procedures utilized the decrease either in the absorbance of the charge-transfer band (Table I) or in the arene concentration (by GC analysis with an appropriate alkane as the internal standard).

Formation Constants of the EDA Complexes of Arenes and OsO_4. In a typical experiment, a 3.0-mL aliquot of a standard solution of OsO_4 in the appropriate solvent (ca. 8 mM) was transferred to a 1-cm quartz curvette equipped with a stirrer bar. The UV–vis spectrum was measured with a sample of pure solvent as the reference. This spectrum served as a base line for the subsequent measurements. A known amount of arene was added, and the solution thoroughly mixed. The spectrum was remeasured, and the absorbances (A_{CT}) at three different wavelengths close to λ_{max} were noted. This procedure was repeated at least seven times. From a plot of $[OsO_4]/A_{CT}$ against $[arene]^{-1}$ the slope was estimated as $(K\epsilon_{CT})^{-1}$ and the intercept as ϵ_{CT}^{-1}.

X-ray Crystallography of OsO_4 Adducts to Benzene and Anthracene. The 2:1 benzene adduct B of approximate dimensions 0.80 × 0.50 × 0.20 mm was mounted in a random orientation on a Nicolet R3m/V automatic diffractometer. The radiation used was Mo Kα monochromatized by a highly ordered graphite crystal. Final cell constants as well as other information pertinent to data collection and refinement were space group, $P\bar{1}$ (triclinic); cell constants, a = 12.299 (6) Å, b = 13.318 (8) Å, c = 14.298 (8) Å, α = 92.46 (4)°, β = 114.65 (4)°, γ = 115.10 (4)°, V = 1858 Å^3; molecular formula, $C_{26}H_{26}N_4O_8Os_2 \cdot CH_2Cl_2$; formula weight, 987.9; formula units per cell, Z = 2; density, ρ = 1.77 g cm^{-3}; absorption coefficient, μ = 70.3 cm^{-1}; radiation (Mo Kα), λ = 0.71073 Å; collection range, $4° < 2\theta < 35°$; scan width, $\Delta\theta = 1.7 + (K\alpha_2 - K\alpha_1)°$; scan speed range, 3.0–15.0° min^{-1}; total data collected, 2308; independent data, $I > 3\sigma(I)$, 1747. The Laue symmetry was determined to be $\bar{1}$, and the space group was shown to be either $P1$ or $P\bar{1}$. Intensities were measured by using the ω scan technique, with the scan rate depending on the count obtained in rapid prescans of each reflection. Two standard reflections were monitored after every 2 h or every 100 data collected, and these showed linear isotropic decay amounting to 75% over the 36-h course of the experiment. In reducing the data, Lorentz and polarization corrections were applied as well as an empirical absorption correction based on ψ scans of nine reflections having χ values greater than 70°. The structure was solved by use of the SHELXTL Patterson interpretation program, which revealed the positions of the two Os atoms in the asymmetric unit, which comprises one full molecule. The remaining non-hydrogen atoms were located in subsequent difference Fourier syntheses. Since there were not very many observed data, each of the pyridine rings was treated as a rigid body, modeled on the accurately refined results of a previously determined organometallic structure. Separate isotropic thermal parameters were refined for each atom. One of the rings (N2) was found to have unusually high thermal motion and was quickly found to be disordered over two sites at roughly right-angles to each other about a common pivot. When the thermal parameters involved were constrained to similar values as the other pyridines, the population factors refined to 65%:35% for the N2:N2′ rings, respectively. All remaining atoms were converted to anisotropic motion, after which all hydrogens were entered in ideal calculated positions. A single isotropic temperature factor was used for all of the hydrogen atoms. At this point, an area of disordered solvent was found and determined to be composed of three separate molecules. All appear to be methylene chloride and are refined to occupancy factors of approximately 40%, 30%, and 35% for C27, C28, and C29, respectively. Due to the low populations rigid bodies were used, based on the best positioning of the C27 unit. After all shift/esd ratios were less than 0.5, convergence was reached at the agreement factors: $R = \sum||F_o| - |F_c||/\sum|F_o|$, 0.068; $R_w = [\sum w(|F_o| - |F_c|)^2/\sum w|F_o|^2]^{1/2}$, 0.058; weights, $w = \sigma(F)^{-2}$. No unusually high correlations were noted between any of the variables in the last cycle of full-matrix least-squares refinement, and the final difference density map showed a maximum peak of 1.4 e/Å^3, positioned 1.3 Å from Os2. All calculations were made with Nicolet's SHELXTL PLUS (1987) series of crystallography programs.

The 2:1 anthracene adduct A of dimensions 0.75 × 0.35 × 0.20 mm was mounted in random orientation of the diffractometer as described above. Final cell constants as well as other information pertinent to the crystallography were as follows: space group, $P\bar{1}$, triclinic; cell constants, a = 12.184 (4) Å, b = 12.633 (4) Å, c = 15.372 (6) Å, α = 88.34 (3)°, β = 89.38 (3), γ = 87.55 (3); V = 2363 Å^3; molecular formula, $C_{34}H_{30}N_4O_8Os_2 \cdot 3.5CH_2Cl_2$; formula weight, 1300.3; formula units per cell, Z = 2; density, ρ = 1.83 g cm^{-3}; absorption coefficient, μ = 58.3 cm^{-1};

(89) The emergent white light consisted of an uniform continuum in the spectral range between 450 and 780 nm.

(90) For a full description of the instrumentation, see: Atherton, S. J.; Hubig, S. M.; Callan, T. J.; Duncanson, J. A.; Snowden, P. T.; Rodgers, M. A. J. *J. Phys. Chem.* **1987**, *91*, 3137.

radiation (Mo Kα), λ = 0.71073 Å; collection range, 4° < 2θ < 40°; scan width, $\Delta\theta = 1.4 + (K\alpha_2 - K\alpha_1)°$; scan speed range, 3.0–15.0° min^{-1}; total data collected, 4426; independent data, $I > 3\sigma(I)$, 3637. The Laue symmetry was determined to be $\bar{1}$, and the space group was shown to be either $P1$ or $P\bar{1}$. Intensities were measured with the ω scan technique as described above. In reducing the data, Lorentz and polarization corrections were applied as well as an empirical absorption correction based on ψ scans of ten reflections having χ values between 70 and 90°. The structure was solved by use of the SHELXTL Patterson interpretation program, which revealed the positions of the two Os atoms in the asymmetric unit, which comprise one full molecule. The remaining non-hydrogen atoms were located in subsequent difference Fourier syntheses. One of the rings (N2) was found to have unusually high thermal motion and was quickly found to be disordered over two sites at roughly 35° to each other about a nearly common pivot. When the thermal parameters involved were constrained to similar values as the other pyridines, the population factors refined to 65%:35% for the N2:N2′ rings, respectively. Ideal rigid body phenyl rings with fixed isotropic temperature factors were used for the N2 and N2′ rings. All remaining atoms were converted to anisotropic motion, after which all hydrogens were entered in ideal calculated positions. A single nonvariable isotropic temperature factor was used for all of the hydrogen atoms. At this point, four areas of disordered solvent were found and determined to be composed of nine discernable orientations of methylene chloride. The C35 area had only one orientation (80% occupancy), the C36 area had three orientations (40%/30%/30%), the C37 area had two (40%/30%), and the C38 area had three (40%/30%/30%). Thus, there were a total of 3.5 molecules of solvent, statistically, for every solute molecule in the crystal. Due to the low populations rigid bodies were used, based on the geometry of an ordered molecule found in a previous structure. No attempt was made to include solvent hydrogens. After all shift/esd ratios were less than 0.2, convergence was reached at the agreement factors: $R = \sum||F_o| - |F_c||/\sum|F_o|$, 0.044; $R_w = [\sum w(|F_o| - |F_c|)^2/\sum w|F_o|^2]^{1/2}$, 0.046. No unusually high correlations were noted between any of the variables in the last cycle of full-matrix least-squares refinement (except the disordered solvent molecules), and the final difference density map showed a maximum peak of about 1 e/Å^3, positioned within one of the solvent groups. The atomic coordinates and equivalent isotropic thermal parameters as well as the observed and calculated structure factors for B and A are included in the Supplementary Material.

Promoted Thermal Osmylation of 9-Methylanthracene Dimer. 9-Methylanthracene dimer (10.5 mg, 2.73×10^{-5} mol), osmium tetroxide (28 mg, 1.1×10^{-4} mol) and pyridine (2.2×10^{-4} mol) were dissolved in heptane (3 mL), and the solution was sealed in an ampoule in vacuo. The mixture was heated to 60 °C for 18 h and then at 100 °C for a further 26 h in the dark. The solvent was removed under reduced pressure. The mixture was analyzed by ^{1}H NMR ($CDCl_3$) to give 31% 9-methylanthracene, 40% unreacted dimer, and 29% of the anti-isomer of the adduct A_m. To test for the thermal cracking, 9-methylanthracene dimer (10.2 mg, 2.7×10^{-5} mol) and heptane (3 mL) were sealed in an ampoule in vacuo, and the solution was heated to 100 °C in the dark for 48 h. Spectrophotometric analysis of the resulting solution indicated the presence of unreacted dimer (1.2×10^{-5} mol) and 9-methylanthracene (3.0×10^{-5} mol). We conclude that 56% of the dimer was converted to the monomer. In order to test for the thermal reaction of OsO_4 with pyridine, osmium tetroxide (28 mg, 0.11 mmol) and pyridine (18 L, 0.22 mmol) were dissolved in heptane (3 mL), and the solution was sealed in an ampoule in vacuo. The yellow solution was heated to 100 °C in the dark for 48 h. Iodometry of the final pale yellow solution indicated that only 10.2 mg of OsO_4 (36%) remained unreacted.

Acknowledgment. We thank the National Science Foundation and the R. A. Welch Foundation for financial support, J. D. Korp for crystallographic assistance, the Center for Fast Kinetics Research (under the auspices of NIH Grant RR00886 and the University of Texas, Austin) for use of their picosecond laser flash photolysis equipment, and funds from the National Science Foundation to construct our ns-μs laser flash system at Houston.

Supplementary Material Available: Table II containing formation constants of [Ar, OsO_4] complexes by the Benesi–Hildebrand method and Tables A–D and F–I containing X-ray crystallographic data consisting of atomic coordinates and equivalent isotropic displacement parameters, bond angles and lengths, and anisotropic displacement parameters for the benzene and anthracene adducts **B** and **A**, respectively (8 pages); Tables E and J containing observed and calculated structure factors (19 pages). Ordering information is given on any current masthead page.

Primary Deuterium Kinetic Isotope Effects for the Thermal [1,7] Sigmatropic Rearrangement of 7-Methylocta-1,3(*Z*),5(*Z*)-triene

John E. Baldwin* and V. Prakash Reddy

Contribution from the Department of Chemistry, Syracuse University, Syracuse, New York 13244. *Received June 2, 1988*

Abstract: 7-Methylocta-1,3(*Z*),5(*Z*)-triene isomerizes to 2-methylocta-2,4(*Z*),6(*Z*)-triene over the temperature range 60–115 °C through a first-order process characterized kinetically by the activation parameters log $A^H = 9.8$ and $E_a^H = 21.5$ kcal/mol. Parallel kinetic work with the 7-deuterio-7-methyloctatriene establishes the Arrhenius parameters log $A^D = 10.3$ and $E_a^D = 23.5$ kcal/mol. Thus $A^D/A^H = 3.2$ and $(E_a^D - E_a^H) = 2.0$ kcal/mol, and a substantial tunneling component for the [1,7] sigmatropic hydrogen migration is evident.

Primary deuterium kinetic isotope effects for sigmatropic migrations of hydrogen have attracted renewed attention in the past few years. The magnitudes k_H/k_D and the possible temperature dependences of these ratios of rate constants continue to attract interest and present substantial challenges to both experimentalists and theoreticians. While most of this attention has been devoted to [1,5] hydrogen shifts,[1-4] the magnitudes of several [1,7] hydrogen migrations have been reported. The [1,7] sigmatropic isomerizations leading from 1,3(*Z*),5(*Z*)-octatriene to two isomers of 2,4,6-octatriene exhibit k_H/k_D values of 6.4–7.7.[5] For two *cis*-isotachysterol analogues,[6] [1,7] hydrogen shifts were found to have primary k_H/k_D values of 4.0 and 2.6 at 98.4 °C, and two previtamin D analogues gave the corresponding vitamin D analogues at 80.4 °C with k_H/k_D values of about 6.[7] A much

(1) Jensen, F.; Houk, K. N. *J. Am. Chem. Soc.* **1987**, *109*, 3139–3140.
(2) Gajewski, J. J. *Isotopes in Organic Chemistry*; Buncel, E., Lee, C. C., Eds.; Elsevier: Amsterdam, 1987; Vol 7, pp 115–176.
(3) Shen, G.-Y.; Tapia, R.; Okamura, W. H. *J. Am. Chem. Soc.* **1987**, *109*, 7499–7506 and references therein.
(4) Dewar, M. J. S.; Healy, E. F.; Ruiz, J. M. *J. Am. Chem. Soc.* **1988**, *110*, 2666–2667.
(5) Baldwin, J. E.; Reddy, V. P. *J. Am. Chem. Soc.* **1987**, *109*, 8051–8056.
(6) Hoeger, C. A.; Johnson, A. D.; Okamura, W. H. *J. Am. Chem. Soc.* **1987**, *109*, 4690–4698.

0002-7863/88/1510-8223$01.50/0